

Catalysis

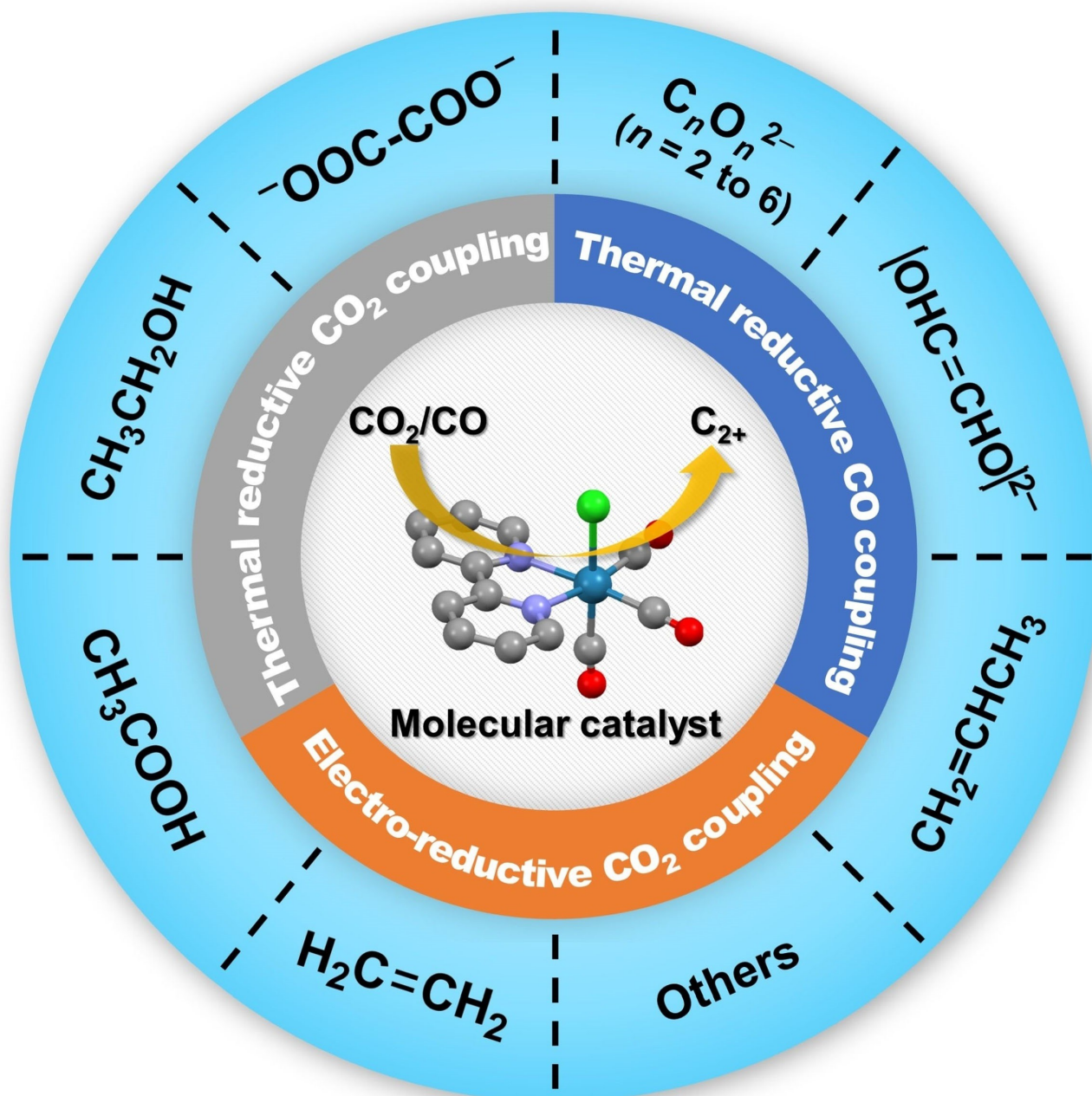
How to cite: *Angew. Chem. Int. Ed.* **2022**, *61*, e202200723

International Edition: doi.org/10.1002/anie.202200723

German Edition: doi.org/10.1002/ange.202200723

Molecular Catalysts for the Reductive Homocoupling of CO₂ towards C₂₊ Compounds

Hong-Qing Liang,* Torsten Beweries,* Robert Francke,* and Matthias Beller*



CO₂ and CO homocouplings to multi-carbon compounds mediated by molecular catalysts are reviewed in this article. Both thermochemical and electrochemical reductive approaches are discussed in detail.

Abstract: The conversion of CO₂ into multicarbon (C₂₊) compounds by reductive homocoupling offers the possibility to transform renewable energy into chemical energy carriers and thereby create “carbon-neutral” fuels or other valuable products. Most available studies have employed heterogeneous metallic catalysts, but the use of molecular catalysts is still underexplored. However, several studies have already demonstrated the great potential of the molecular approach, namely, the possibility to gain a deep mechanistic understanding and a more precise control of the product selectivity. This Minireview summarizes recent progress in both the thermo- and electrochemical reductive homocoupling of CO₂ toward C₂₊ products mediated by molecular catalysts. In addition, reductive CO homocoupling is discussed as a model for the further conversion of intermediates obtained from CO₂ reduction, which may serve as a source of inspiration for developing novel molecular catalysts in the future.

1. Introduction

The excessive utilization of fossil fuels has led to a rapid rise in the atmospheric carbon dioxide (CO₂) level since the industrial revolution, which has triggered environmental issues (e.g. green-house effect and rise in sea levels) and energy crises.^[1] To mitigate the carbon footprint, the valorization of CO₂ into value-added products is of fundamental interest. As a consequence of the thermodynamic stability of CO₂, a high energy input is required for the activation and transformation of CO₂. Industrial processes for the upgrading of C₁ chemicals, for example Fischer–Tropsch and CO₂ cycloaddition processes, usually proceed under drastic reaction conditions (high temperatures of > 100 °C and high pressure of 5–20 bar) and suffer from low selectivity, which makes high capital investment necessary and requires additional purification steps to obtain the desired products. As a promising candidate, the reductive homocoupling of CO₂ combined with renewable energy and electrochemistry offers an economically and environmentally attractive strategy to convert CO₂ into value-added multicarbon (C₂₊) compounds. The C₂₊ products, for example, ethylene, ethanol, acetate, and higher alcohols or alkanes, possess higher energy densities and larger market sizes than C₁ products.^[2] Their production could significantly reduce global demands for fossil feedstocks and close the anthropogenic carbon cycle. In addition, the upgrading of CO₂ to C₂₊ feedstocks by carbon–carbon (C–C) coupling provides avenues to efficiently store renewable energy in chemical energy carriers, which is the key to power-to-X and artificial photosynthesis technologies.^[3]

A variety of in-depth studies have been carried out on heterogeneous metallic catalysts, with many of them show-

ing favorable activities for the formation of C–C bonds.^[4] However, when studying such systems, one usually encounters difficulties in identifying active sites and understanding the mechanistic pathways. Furthermore, the selective reduction of CO₂ to a specific product is a major challenge. As an alternative, molecular catalysts possess well-defined active centers, thereby allowing the establishment of a precise structural model and understanding of the underlying mechanisms.

The chemical one-electron reduction of CO₂ with molecular catalysts enables a symmetric coupling of two CO₂ molecules to form the oxalate anion, which is considered the simplest CO₂ coupling reaction (Figure 1).^[5] Recent progress in the electrochemical CO₂ reduction reaction (eCO₂RR) has led to the generation of more highly reduced products such as acetic acid and ethanol.^[6] Previously reported molecular catalysts, especially earth-abundant metal complexes, have shown excellent performance for the eCO₂RR, with a Faradaic efficiency (FE) towards carbon monoxide (CO) and formic acid close to unity.^[7] Along with the progress in the design of molecular catalytic systems, a

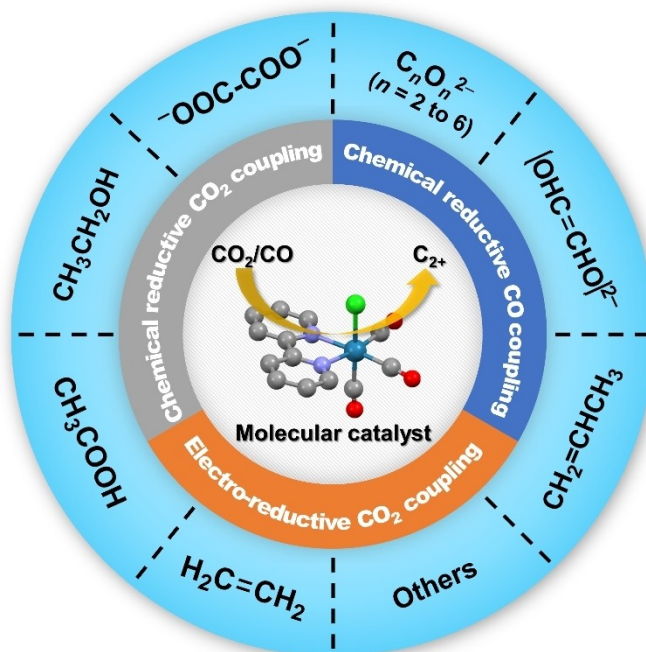


Figure 1. Schematic representation of the scope of this Minireview.

[*] H.-Q. Liang, T. Beweries, R. Francke, M. Beller
Leibniz-Institute for Catalysis
Albert-Einstein-Strasse 29a
18059 Rostock (Germany)
E-mail: hongqing.liang@catalysis.de
torsten.beweries@catalysis.de
robert.francke@catalysis.de
matthias.beller@catalysis.de

© 2022 The Authors. Angewandte Chemie International Edition published by Wiley-VCH GmbH. This is an open access article under the terms of the Creative Commons Attribution Non-Commercial License, which permits use, distribution and reproduction in any medium, provided the original work is properly cited and is not used for commercial purposes.

series of studies have recently been published in which CO₂ is electrochemically reduced to C₂₊ products using molecular catalysts.^[8] Although the performances are not yet satisfactory for technical-scale applications, the possibility to tune the catalyst structure as well as the utilization of novel immobilization methods pave the way toward reaction optimization.

In the context of the direct coupling of CO₂ to C₂₊ compounds, the coupling of CO, a readily available two-electron reduction product from CO₂, is also of great interest, as it forms a part of possible consecutive CO₂-to-C₂₊ pathways. Notably, the electrochemical reduction of CO has shown tremendous activity and selectivity to C₂₊ products.^[9] However, currently it can only be achieved with metallic Cu electrodes. In contrast, studies on the chemical reduction of CO in the presence of suitable molecular catalysts have revealed a wide range of coupling reaction patterns, including reductive dimerization or oligomerization, cyclooligomerization, hydrogenative coupling, hydrodeoxygenative coupling, and hydrocyclootrimerization.^[10] Thus, numerous dimerization and oligomerization products could be generated (Figure 1), which greatly broadens the potential range of products obtainable from CO₂ reduction.

Although many excellent review papers on the eCO₂RR using molecular catalysts have been published, most of them focus on the generation of C₁ products.^[11] In this Minireview, we turn our focus to reductive homocoupling reactions of

CO₂ that are facilitated by molecular catalysts and lead to the generation of C₂₊ products. Both electrochemical and thermochemical processes are considered, to discuss the similarities and differences. In addition, reductive CO homocoupling will also be included, which will inspire the development of novel molecular catalysts for CO₂ coupling. Finally, we will give our point of view on the most promising strategies to promote C–C coupling processes, which may boost the further development of molecular catalysts for CO₂ reduction in the future.

2. Mechanistic Pathways for C–C Coupling

Despite the apparent simplicity, the reductive homocoupling of CO₂ can be a highly complex process, depending on the catalyst and the reaction conditions, and involves the transfer of multiple electrons and often multiple protons. Both the activation of CO₂ and the formation of the C–C bond(s) between C₁ intermediates are challenging key steps toward the generation of multicarbon products. CO₂ is a highly stable and chemically inert molecule, because of its strong chemical bonds and linear geometric structure. Therefore, the reduction of CO₂ to CO₂^{•-} is difficult, and requires a very negative redox potential ($E = -1.90$ V vs. standard hydrogen electrode (SHE)).^[12] This unfavorable radical anion intermediate often turns the activation process into



Hong-Qing Liang received his BSc (2011) and PhD (2016) from Zhejiang University, under the supervision of Prof. Z.-K. Xu. He then carried out postdoctoral research at the University of Texas at San Antonio (2016–2018, with Prof. B. Chen), Aarhus University (2018–2019, with Prof. K. Daasbjerg), and University of Padova (2020–2021, with Prof. S. Agnoli). Currently, he is an Alexander von Humboldt fellow at Leibniz Institute for Catalysis in the group of Prof. M. Beller. His research focuses on novel catalytic systems for electrochemical CO₂

reduction to C₂₊ products.



Torsten Beweries studied chemistry at the University of Rostock and carried out diploma and PhD studies at the Leibniz Institute for Catalysis (advised by Prof. U. Rosenthal). After postdoctoral research with Prof. R. N. Perutz (University of York, UK) in 2009, he returned to LIKAT, where he established his own research group. After completing his habilitation in 2016, he became head of the research department "Coordination Chemistry and Catalysis" at LIKAT. His research is focused on stoichiometric, catalytic, and mechanistic aspects of small molecule

activation using organometallic systems based on Group 4 and 9 metals.



Robert Francke studied chemistry at Bonn University (Germany) and Alicante University (Spain). In 2012, he completed his PhD with Prof. S. Waldvogel at Mainz University (Germany). He then joined the group of Prof. R. D. Little at the University of California Santa Barbara as a Feodor Lynen Fellow (Alexander von Humboldt Foundation). In 2014, he started his independent career at Rostock University with a Liebig Fellowship (Fonds der Chemischen Industrie). After his habilitation in 2020 and with financial support through the Heisenberg Program (German Research Foundation), he joined the Leibniz Institute for Catalysis, where he currently leads the research department "Electrochemistry & Catalysis".



Matthias Beller, born in Gudensberg (Germany) in 1962, obtained his PhD in 1989 with Prof. L. F. Tietze at the University of Göttingen. After postdoctoral research with Prof. B. Sharpless at MIT (USA), he worked at Hoechst AG in Frankfurt (1991–1995), before starting his own academic career at TU Munich. In 1998, he relocated to Rostock to head the Leibniz-Institute for Catalysis. He is also Vice-president of the Leibniz Association and a member of 3 German Academies of Sciences including the German National Academia "Leopoldina".

His research focuses on homogeneous and heterogeneous catalysts for the sustainable synthesis of fine/bulk chemicals as well as energy technologies.

the bottleneck of the reaction. In many catalytic mechanisms, especially those leading to C_1 products, this high-energy intermediate is bypassed and, instead, CO_2 activation proceeds through a polar mechanism (e.g. by nucleophilic attack of a metal center in a low oxidation state at the carbon atom). However, for most coupling scenarios, $CO_2^{\bullet-}$ is considered to be involved as an intermediate.

In the case of thermoreductive couplings that involve activation by metal complexes, the conversion of CO_2 usually takes place under aprotic conditions and generates oxalate as the only C_{2+} product. The C–C coupling may proceed through two different pathways, as shown in Figure 2. A frequently proposed pathway follows a diradical coupling mechanism. CO_2 is first activated to form the $CO_2^{\bullet-}$ radical anion by one-electron reduction with the aid of a metal complex. The $CO_2^{\bullet-}$ radical anion is likely to be coordinated to the oxidized metal complex, thereby forming the $[L-M]^+[CO_2]^{\bullet-}$ intermediate **I**. Then, two molecules of the intermediates recombine to form oxalate complex **II** (Figure 2A).^[13] Recently, a new mechanism was proposed on the basis of density functional theory (DFT) studies of a dinuclear Cu complex.^[14] As shown in Figure 2B, one CO_2 molecule is first coordinated between two metal centers and reduced cooperatively by both metals, thereby leading to a fully delocalized mixed-valence $[L-M]^+[CO_2]^{\bullet-}[M-L]$ radical anion intermediate **III**. The metal-ligated CO_2 molecule is further partially reduced, which is followed by nucleophilic-like attack at the carbon atom of the second metal-coordinated CO_2 molecule (**IV**). Finally, oxalate complex **II** is generated. Generally, the diradical coupling mechanism is assumed to be the favored pathway when active species with electron-rich metal centers are involved, because of the strong coordination tendency between $CO_2^{\bullet-}$ and the oxidized metal complex. The second pathway in Figure 2B may apply to electron-deficient metal complexes. At the present stage, it is generally difficult to distinguish between these two mechanistic pathways, which is why further investigations are needed.

At this point, it is also worthwhile looking at electrochemical CO_2 coupling on catalytically active electrodes (see Figure 2, bottom). Even though these are heterogeneous processes, some of the occurring intermediates may also be interesting targets for homogeneous catalytic studies. The mechanistic situation becomes relatively complex because of the participation of protons in the reaction sequence. After activation of CO_2 , the formed $*CO_2^{\bullet-}$ intermediate undergoes a protonation process to form $*COOH$. Further hydrogenation and dehydration leads to the formation of $*CO$, which is considered a key intermediate in the formation of C_{2+} products by the eCO_2RR .^[15] New C_1 intermediates such as $*CHO$ and $*COH$ are subsequently formed through $*CO$ hydrogenation. Consequently, various C_1 intermediates including $*CO$, $*COH$, $*CHO$, etc. can be generated through several proton-coupled electron-transfer (PCET)

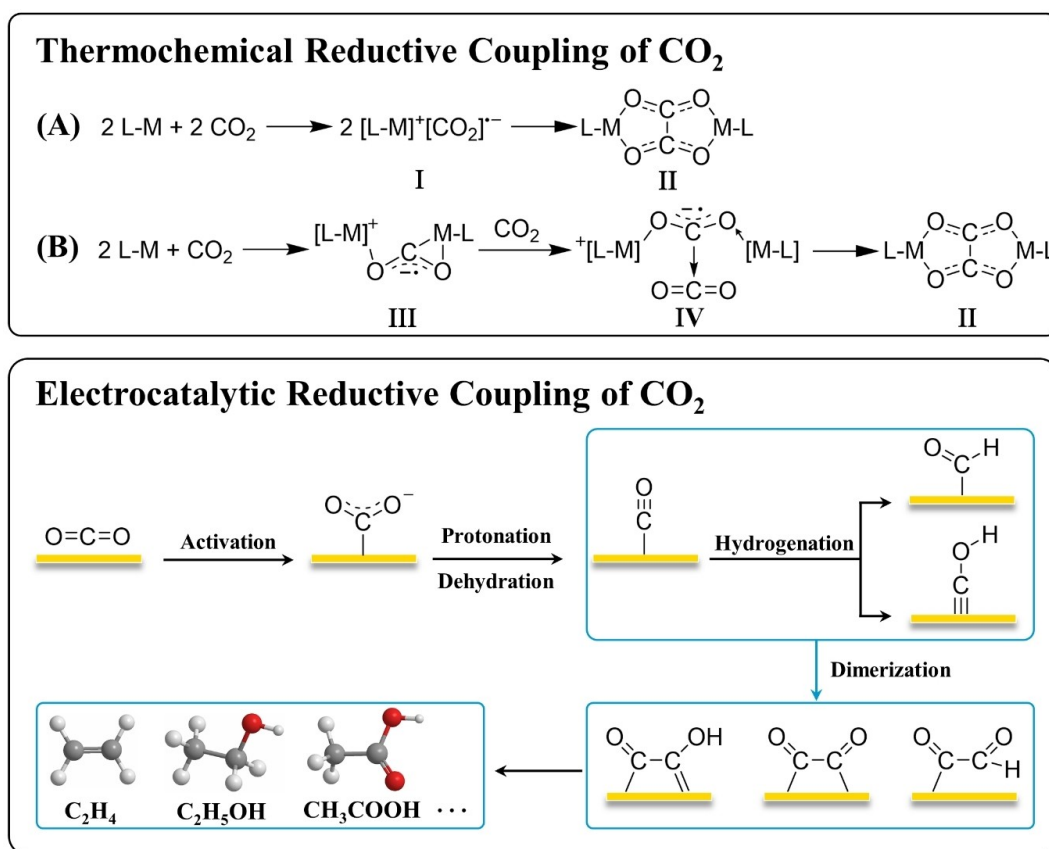


Figure 2. Mechanistic pathways for CO_2 coupling induced by chemical and electrocatalytic reduction.

steps. Considering that the conversion of C_1 intermediates (such as *CO , *CHO and *COH) into C_{2+} products is a very complex process involving numerous PCET steps, here we only introduce some representative coupling pathways.^[16] The dimerization of the *CO , *CHO , and *COH intermediates generate *COCO , *COCHO , and *COCOHO , which are key intermediates for C_{2+} products. Whereas *COCO is formed by the dimerization of *CO ,^[17] *COCHO and *COCOHO can be formed either through the direct dimerization of *CO with *CHO and *COH , respectively, or the further hydrogenation of *COCO .^[18] Depending on the experimental conditions (e.g. catalyst properties, reaction medium, applied potentials), these C_2 intermediates then react with protons and/or electrons to produce various C_2 reduction products, for example, C_2H_4 , C_2H_5OH , and CH_3COOH .^[19] Considering that all these pathways are proton-assisted, it is clear that proton availability plays a crucial role in several respects. In addition to the influence of the thermodynamics and kinetics of the coupling reactions (and other eCO_2RR processes), it must also be taken into account that the proton reduction itself can compete with the desired reaction. Optimization of the pH value is, therefore, of great importance in the development of efficient electrocatalytic processes (for details regarding the role of protons in eCO_2RR , see Ref. [11]).

Although comprehensive studies have been conducted on the C–C coupling mechanisms of the eCO_2RR , it should be noted that most of them focus on the use of Cu electrodes, which are particularly efficient due to the moderate absorption energy of *CO .^[15] Although some of these heterogeneous pathways are clearly not applicable to molecular catalysts, the proposed catalytic schemes may still be considered as a source of inspiration for the design of new homogeneous processes. Regarding the already-existing

molecular catalysts for CO_2 -to- C_{2+} conversions, an improved understanding of the underlying mechanisms is crucial for a knowledge-based optimization toward processes with competitive performances.

3. CO_2 Activation for Thermoreductive Coupling

In 1983, the first molecular reductive coupling of CO_2 was reported using a cyclopentadienyl Ti^{III} alkyl dimer, although with low selectivity (Figure 3B1),^[20] and subsequently there have been several reports of similar transformations utilizing f-block metal complexes and reduced transition-metal complexes. The f-block metals are in general more oxophilic, thereby enabling a stronger oxalate coordination. Consequently, a bridging oxalate complex is usually formed as the product, from which the liberation of oxalate is very difficult and hence the development of a real catalytic process is intrinsically problematic. In contrast, oxalate can easily be removed from the reduced transition-metal complexes with the help of a lithium salt additive or KC_8 , which generates insoluble $C_2O_4^{2-}$ salts, potentially opening the opportunity for establishing catalytic cycles.^[14b,21] However, most of the thermoreductive CO_2 coupling reactions that involve activation by metal complexes are stoichiometric reactions rather than catalytic processes. To our knowledge, only one example reported by Murray and co-workers could be considered truly catalytic, with a turnover number (TON) of 24.^[22] In addition, both complexes suffer from competitive reductive disproportionation to CO and CO_3^{2-} , thus lowering the selectivity for CO_2 coupling to oxalate. The formation of the oxalate complex is thermodynamically more favorable than the corresponding CO and CO_3^{2-}

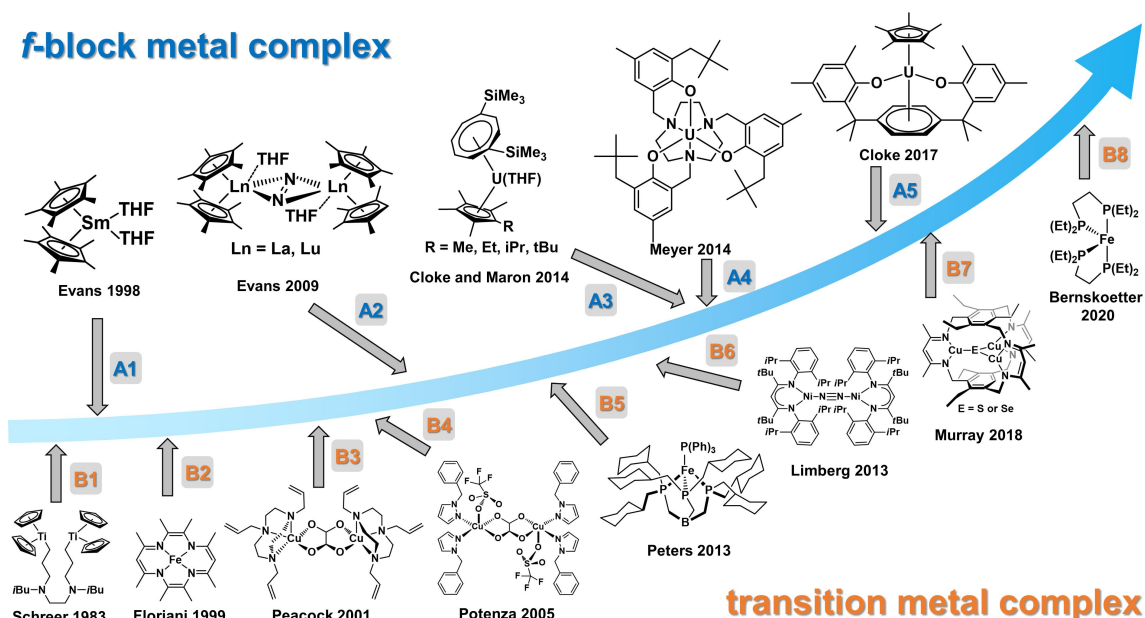


Figure 3. Evolution of molecular systems for the reductive coupling of CO_2 to oxalate. Series A represents f-block metal complexes, while series B includes transition-metal (Ti, Cu, Fe, Ni) complexes.

complexes.^[23] Nevertheless, the nature of the coupling as a bimolecular process makes it kinetically disadvantageous.

The reductive coupling of CO₂ to oxalate is a challenging but also a very meaningful transformation, as oxalate is an important feedstock for the synthesis of some useful chemical commodities, such as ethylene glycol and methyl glycolate.^[24] To favor the conversion of CO₂ into oxalate, careful consideration has to be given to modulate the steric effect of the ligands and adopt proper reaction conditions (solvent and temperature).

Evans et al. found that the reaction of the organo-samarium complex (C₅Me₅)₂Sm(THF)₂ (Figure 3A1) with CO₂ in THF at room temperature leads to the formation of the oxalate-bridged complex [(C₅Me₅)₂Sm(THF)₂](μ-η²:η²-O₂CCO₂) in greater than 90 % yield (calculated, as in the following examples, with respect to the amount of employed metal complex).^[15] The strong reducing power of (C₅Me₅)₂Sm(THF)₂ and its large oxophilicity facilitate the coupling reaction. The authors then further evaluated the influence of the lanthanide (Ln) metal size on the reduction of CO₂ using [(C₅Me₄H)₂Ln(THF)₂](μ-η²:η²-N₂) complexes (Figure 3A2).^[25] The results reveal that the complex with the smallest Ln ion, Lu³⁺, selectively reacts with CO₂ to generate the corresponding oxalate complex in 95 % yield, whereas the complex with the largest Ln ion, La³⁺, allows the insertion of CO₂ into multiple sites and thus formation of diverse products. Later, Cloke, Maron, and co-workers extended the reaction to organoactinides,^[23] and demonstrated the crucial role of steric control in the selective generation of the oxalate complex, by using a series of U^{III} mixed sandwich complexes (Figure 3A3). Whereas the products are the bridging oxo complex and the bridging oxalate complex when R=Me, bridging carbonate and bridging oxalate complexes are formed for R=Et or ⁱPr. Notably, when using the complex with R=^tBu, the sole product is a bridging carbonate complex. Thus, it appears that steric influences determine the reductive pathways.

Meyer and co-workers reported the formation of oxalate in moderate yield (48 %) with the aid of KC₈ when [(^{neopentyl},^{methyl}ArO)₃tacn)U] (tacn=triazacyclononane) was reacted with CO₂ (Figure 3A4).^[26] The Cloke group further found that the selectivity for the reduction of CO₂ is temperature-dependent in the case of [U(Cp*)(*p*-Me₂bp)] (*p*-Me₂bp=C₆H₄(*p*-C-(CH₃)₂C₆H₃Me₂O⁻)₂) (Figure 3A5): at low temperatures (-78 °C) oxalate formation is favored, while at room temperature carbonate is the dominant product.^[27]

In addition to f-block metals, transition-metal (Cu, Fe, Ni) complexes with low metal oxidation states are also capable of activating CO₂ by internal electron transfer. The first Fe complex that was reported to generate oxalate, although only as a minor product, is Fe^Idibenzotetramethyl-tetra[14]azaannulene (Figure 3B2).^[28] Cu^I complexes, for example, Cu(triallyl-1,4,7-triazacyclononane) (Figure 3B3) and Cu[bis(1-benzyl-1*H*-pyrazole)](trifluoromethanesulfonato) (Figure 3B4),^[5,29] were subsequently reported that can selectively generate an oxalate-bridged complex. Later, the Peters group reported a [PhBP₃^{CH₂Cy}]Fe(PPh₃) complex, which is capable of reductive coupling CO₂ to oxalate in 70 % yield (Figure 3B5).^[30] They demonstrated the key role

of the capping phosphine ligand and coordinating solvent in achieving reductive coupling instead of the reductive disproportionation of CO₂. The generation of a bridging-oxalate complex is favored in the presence of the capping phosphine ligand when a more strongly coordinating solvent is used. Otherwise, the [(PhBP₃^{CH₂Cy})Fe]₂(μ-O)(μ-CO) complex, the product of a partial decarbonylation, is preferentially formed. In addition, a Ni-based complex, [L^{tBu}Ni^I(N₂)Ni^IL^{tBu}] (L^{tBu}=[HC(C(*t*Bu)NC₆H₃(*i*Pr)₂)₂]⁻), can also mediate the reductive coupling of CO₂ to oxalate, although with a lower yield of 20 % (Figure 3B6).^[21] The complex Cu₃EL (L³⁻=tris(β-diketiminato)cyclophane, E=S, Se) proposed by the Murray group exhibits the highest TON of 24 reported thus far, with an oxalate yield of 95 % under thermochemical reduction conditions (Figure 3B7).^[22]

A more recently reported Fe⁰ system of the type [(depe)₂Fe] (depe=1,2-bis(diethylphosphino)ethane) afforded oxalate in 98 % yield in the presence of 2 equiv KC₈ in THF at 45 °C (Figure 3B8).^[31] Control experiments using KC₈ only or other Fe-based complexes resulted in lower oxalate yields, thereby demonstrating that the [(depe)₂Fe⁰] species plays a key role in the reductive CO₂ coupling. A further increase in the amount of KC₈ equivalents led to an improved conversion to oxalate with respect to the available Fe complexes (up to 2.1 equiv oxalate per iron); this result led the authors to explicitly point out that a true catalytic process could not be clearly demonstrated.

While f-block and d-block complexes have dominated this field, the development of main group complexes (s-block and p-block) have begun to emerge as a more cost-effective and ecological friendly alternative for CO₂ reductive coupling. Stasch, Jones and coworkers reported that the reactions of magnesium(I) dimers bearing tripodal ligands with excess CO₂ cleanly give carbonate at 60 °C as the thermodynamic product, or oxalate at -60 °C as the kinetic product.^[32] To our knowledge, there is no other precedent for the reductive coupling of CO₂ using main group complexes. However, progress has been made in the disproportionation of CO₂ using amido-digermyne^[33] and dialumene species to produce CO and carbonate,^[34] thus revealing their potential for reductive CO₂ coupling through the design of new ligands and manipulation of the reaction conditions. Certainly, developing complexes of main group elements that are capable of reducing CO₂ toward C₂₊ products represents a promising research field for the future.

4. Electrocatalytic CO₂ Coupling Mediated by Molecular Catalysts

In addition to thermochemical reduction, molecular electrocatalysis has emerged as a promising approach for CO₂ reduction, because of the benign reaction conditions and the possibility to directly use renewable energy. Representative molecular systems for the CO₂RR include Re(bpy)(CO)₃Cl (bpy=2,2'-bipyridine),^[35] Ru(bpy)(CO)₂Cl₂,^[36] Mn(L)(CO)₃Br,^[37] Ir pincer complexes,^[38] iron cyclopentadi-

none complexes^[39] as well as iron and cobalt porphyrins and phthalocyanines.^[40] The corresponding eCO₂RR processes have been studied extensively, whereby the major reduction products turned out to be C₁ compounds, namely, CO and formic acid (or formate).

Recent progress in molecular electrocatalysis has led to the conversion of CO₂ into C₂₊ products, including ethylene, ethanol, acetate, and oxalate. Most of these examples are based on Cu complexes. The distinct feature of Cu compared to other metals is its moderate affinity to *CO, which facilitates the further reductive C–C coupling. Furthermore, catalyst immobilization on the electrode surface has turned out to be a useful strategy to promote coupling pathways. Under appropriate conditions, the generated *CO intermediate can migrate on the surface and dimerize with another *CO molecule, whereas the interaction between two comparable molecular catalytic intermediates in solution may be rather difficult. To achieve a surface-enhanced effect on the catalytic process, a carefully tuned combination of molecular catalyst, support, and immobilization strategy is of great importance.

4.1. Ethylene

Ethylene (C₂H₄) is a widely used chemical feedstock in the polymer industry, particularly in view of polyethylene production, and belongs to the top five chemicals which

impact energy usage and carbon dioxide formation. Nevertheless, the electrochemical reduction of CO₂ to C₂H₄ by molecular catalysts is a nascent subfield, with few examples reported so far. Early studies have demonstrated that trace amounts of C₂H₄ can be produced by eCO₂RR using transition-metal phthalocyanine and porphyrin complexes supported on activated carbon fibers.^[41] Herein, we will only discuss molecular catalytic systems which were reported to render C₂H₄ as one of the major products (FE > 15 %).

In 2016, Brudvig, Wang and co-workers reported that a Cu-porphyrin complex with attached phenolic OH groups (PorCu, Figure 4A) on carbon nanoparticles generated CH₄ and C₂H₄ with FE of 25 % and 17 %, respectively, at –0.98 V vs. reversible hydrogen electrode (RHE). Based on control experiments with copper-free and OH-free porphyrin complexes, it was suggested that both the +1 oxidation state of Cu and the hydroxy group on the porphyrin structure play key roles in determining the performance.^[42] Although the detailed mechanism is not clear, the authors assumed that the Cu center is the active site while the hydroxy group may facilitate the binding of certain reaction intermediates or provide an intramolecular source of protons. Later, crystalline Cu phthalocyanine (CuPc, Figure 4B) immobilized on carbon black was used for eCO₂RR to generate C₂H₄ with FE=25 % and a partial current density of 2.8 mA cm⁻².^[43] Considering the inferior performance of the noncrystalline CuPc, the authors concluded that the close distance between two Cu centers in the crystal

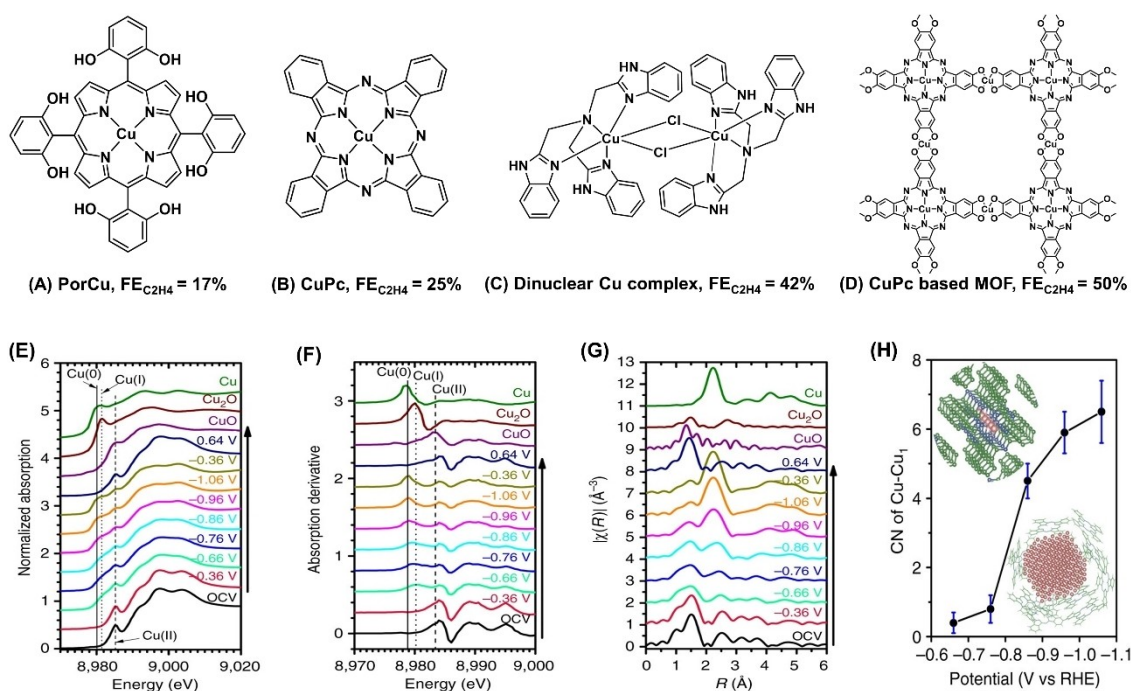


Figure 4. A–D) Reported examples of molecular-based catalysts generating ethylene during eCO₂RR. E–G) In situ XAS measurements on CuPc under electrocatalytic reaction conditions. E) Cu K-edge XANES spectra, F) first-order derivatives of the XANES spectra, and G) Fourier-transformed Cu K-edge EXAFS spectra. H) First-shell Cu–Cu coordination numbers (CNs) of the CuPc catalyst at different potentials. The upper left inset shows the CuPc crystal structure, and the lower right inset illustrates a possible configuration of the Cu nanoclusters generated under the electrocatalytic conditions. Green: C, blue: N, and pink: Cu. Error bars represent the uncertainty of CN determination from the EXAFS analysis (Reprinted from Ref. [50] with permission).

structure is the key factor for the formation of C–C bonds and, consequently, the production of C₂H₄. Inspired by these findings, Nam and co-workers synthesized a dinuclear Cu complex coordinated with the tris(2-benzimidazolylmethyl)-amine ligand (Figure 4C), which possesses a short Cu...Cu distance of 3.77 Å.^[44] Compared with the mononuclear Cu complex, the dinuclear system exhibited a higher selectivity for C₂H₄ (FE = 42 %) at –1.28 V vs. RHE in 0.1 M KCl. Very recently, Liao and co-workers immobilized the CuPc-(OH)₈ complex as a ligand into a two-dimensional metal-organic framework (MOF) with square-planar CuO₄ nodes (Figure 4D).^[45] The as-prepared MOF exhibits an extraordinary performance for eCO₂RR to generate C₂H₄ with a FE of 50 % and a current density of 7.3 mA cm⁻² at –1.2 V vs. RHE in 0.1 M KHCO₃ solution. The enhanced performance is ascribed to the synergistic effect between the CuPc unit and the CuO₄ unit. In contrast to the discrete molecular CuPc, the additional CuO₄ sites provide abundant adsorbed CO molecules which can efficiently migrate to the CuPc sites for C–C bond formation. It is assumed that the energy barrier for the C–C coupling is significantly lowered and the generation of C₂H₄ greatly facilitated, thus opening a new avenue toward designing new supported molecular catalysts for the reductive coupling of CO₂.

It should be noted that most of the molecular catalysts for C₂H₄ generation were immobilized onto a carbon support, for example, carbon black, carbon nanotube, or graphene. Pristine carbon materials generally possess high overpotential for HER,^[46] which makes them a suitable platform for immobilizing molecular catalysts for eCO₂RR. The carbon support also facilitates electron transfer from the electrode to the molecular catalysts, thus enhancing the electrochemical activity.^[47] Furthermore, the porous structure of the carbon support can alter the mass transport from the electrolyte to the electrode, thereby modulating the selectivity and activity of the reaction.^[48] Nam and co-workers found that the dinuclear Cu complex immobilized on graphitized mesoporous carbon exhibited a much higher C₂ product selectivity compared with complexes on carbon nanotubes and graphene oxide.^[44] It was assumed that the porous structure of the carbon support increases the local pH inside the pores compared with the pH of the bulk electrolyte as a result of the limited mass transport, thereby inhibiting the HER and consequently facilitating C–C coupling. A similar selectivity-enhancing effect of the carbon support in protic media has been observed in other studies.^[49]

Despite the progress that was made with molecular catalysts for C–C coupling, special attention should be paid to the stability during electrolysis and the nature of the active site. To illustrate this point, the work on CuPc serves as a cautionary example. A first indication of a changing catalyst structure was given by the fact that C₂H₄ production is achieved in the initial stage (< 10000 s), but continuously decreases and eventually terminates after 12 h. These observations infer a lack of stability of CuPc during the CO₂RR.^[43] To unravel the actual active species responsible for C₂H₄ generation, *in situ* and *operando* X-ray absorption spectroscopy (XAS) was utilized to investigate the evolution

of CuPc under the working conditions (Figure 4E–H).^[50] X-ray absorption near-edge spectroscopy (XANES, Figure 4F) provided information on the oxidation state, geometry, and electronic configuration of the Cu atom, while fitting of extended X-ray absorption fine structure (EXAFS, Figure 4G) data allowed the local coordination environment to be reconstructed. The initial Cu^{II} peak at open circuit voltage (OCV) diminishes and a new Cu⁰ peak dominates in the XANES and EXAFS spectra when the applied potential becomes more negative (Figure 4E–G), which indicates a restructuring of CuPc to form Cu nanoclusters through demetalation of the complexes. The formation of Cu nanoclusters can be further confirmed by the increased Cu–Cu coordination number (CN) as the potential becomes more negative (Figure 4H). It is worth noting that, upon returning to more positive potentials, the Cu⁰ peak disappears and the spectrum is almost identical to the one obtained under the initial OCV conditions, which indicates the reversible formation of Cu nanoclusters. In the study by Nam and co-workers, the formation of copper clusters during catalytic reactions of the dinuclear Cu complex was also observed by bright-field high-resolution transmission electron microscopy (HRTEM).^[44] Although metallic Cu is known to be active for the CO₂RR to generate hydrocarbons, small-sized Cu nanoparticles ($\phi < 5$ nm) usually undergo morphology transformation in the absence of stabilizing additives. These morphology changes lead to the generation of CO and H₂ instead of hydrocarbons, as a result of the increasing number of low-coordinated surface atoms with a strong tendency for the chemisorption of H* and CO₂.^[51] Therefore, Cu nanoclusters stabilized by the ligands are most likely the active species for C–C coupling during the CO₂RR (Figure 4H).

The above-described results obtained with immobilized Cu catalysts provide starting points for the target-oriented manipulation of active sites. On the one hand, efforts should be made to find a long-term-stable Cu complex with a strong metal ion/ligand binding affinity, thus preventing the demetalation process. As a next step, careful optimization of the chemical (ligand functionalization) and spatial (confined space) environments of the Cu complex may lead to further improvements. On the other hand, ligand-stabilized Cu nanoclusters may also be a promising catalytic system for eCO₂RR to C₂₊ products. As reported by Xu et al., a Cu₃ cluster stabilized by graphene-bound hydroxy groups is capable of promoting the production of ethanol.^[52] The challenge is to precisely control the demetalation process of molecular catalysts during electrolysis to form well-defined ligand-stabilized Cu nanoclusters.

4.2. Ethanol

In 2019, Schöffberger, Roy, and co-workers reported a cobalt(III) triphenylphosphine corrole complex with three polyethylene glycol residues attached to the *meso*-aryl groups (Co-corrole, Figure 5A), which is the first molecular catalyst capable of efficiently electroreducing CO₂ to ethanol.^[53] In 0.1 M NaClO₄ (pH = 6.0, 0.1 M phosphate buffer), the Co-corrole-modified carbon paper electrode

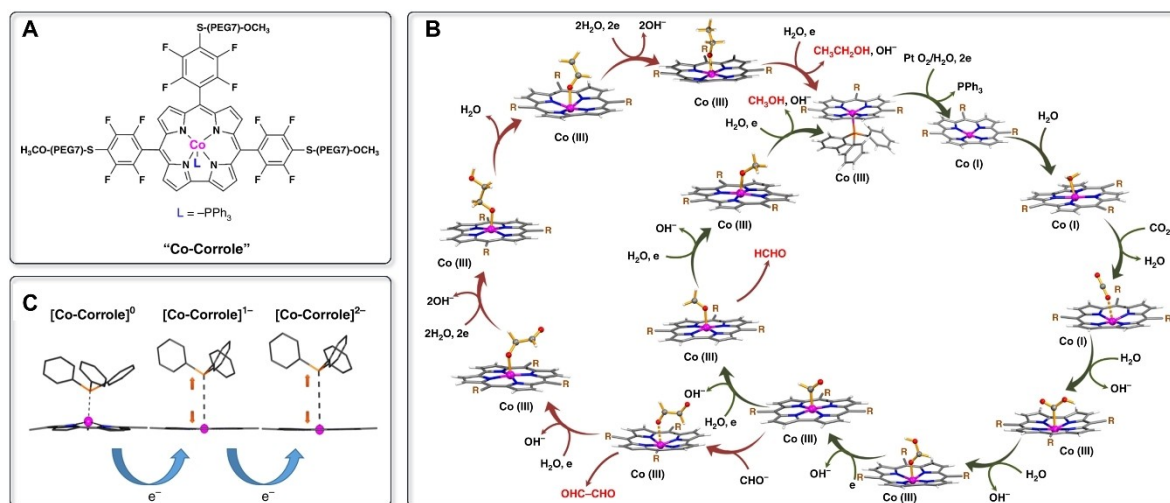


Figure 5. A) Chemical structure of the Co-corrole catalyst. B) Proposed single site mechanism of CO_2 reduction using Co-corrole. C) DFT-optimized geometries of $[\text{Co-corrole}]^0$, $1e^-$ and $2e^-$ -reduced species showing the movement of the Co center into the central cavity of the corrole ring with concomitant lengthening of the Co– PPh_3 bond upon successive reduction (Reprinted from Ref. [53] with permission).

exhibits a FE of 48% toward ethanol production at -0.8 V vs. RHE over a period of 5 h, accompanied by the formation of methanol, acetate, glyoxal, formaldehyde, and formate as by-products. In contrast to the more frequently encountered CO pathway, the authors demonstrated both experimentally and theoretically that the Co-corrole system proceeds through a formic acid pathway (Figure 5B). The formed HCOOH intermediate undergoes a $1e^-$ reduction to give $^*\text{CHO}$ bound to the Co^{III} center. At a low overpotential, $^*\text{CHO}$ is further reduced to CH_3O^* , finally generating methanol. On the other hand, at a more negative potential (< -0.73 V vs. RHE), abundant $^*\text{CHO}$ is generated, which enables the recombination of two formyl radicals to form the glyoxal intermediate (OHC-CHO). Subsequent reduction steps lead to the formation of ethanol. To verify the proposed pathways, formic acid was directly reduced, which yielded a mixture of methanol and ethanol. Similarly, the external addition of 0.1 mM OHC-CHO under the reaction conditions led to ethanol being obtained, thus suggesting OHC-CHO to be a key intermediate for ethanol formation.

The extraordinary selectivity of Co-corrole towards ethanol formation was ascribed to the well-defined structure of the complex. First, the fluorinated *meso*-aryl groups render the corrole ring electron-deficient. Partial loss of the PPh_3 ligand upon one-electron reduction exposes a Co^{II} site, which is further reduced at the applied potential to generate the active Co^{I} center (Figure 5C). The Co–N bonds are thereby reinforced and the π -back bonding enhanced, leading to planarization of the macrocycle. Demetalation is thus inhibited and multiple turnovers per Co center are ensured. Second, the S-PEG(7)-OMe moiety was proposed to play a key role in the $e\text{CO}_2\text{RR}$ process. It is not only supposed to enable the anchoring and uniform distribution of the catalysts across the carbon fibers, but presumably also helps to stabilize the key intermediates at the metal site. Control experiments using two similar Co-corroles with three *meso*- C_6F_5 groups or three *meso*- C_6H_5 groups gener-

ated formic acid, methanol, and acetic acid as major products, with only trace amounts of ethanol, thus demonstrating the significance of both the fluorinated *meso*-aryl groups and the appended S-PEG(7)-OMe moieties.

Despite the report of Co-corrole with a catalyst TON of 196, the electrochemical reduction of CO_2 to ethanol using molecular catalysts alone remains a great challenge. As an alternative, another strategy has recently been developed for cooperative CO_2 -to-ethanol conversion with molecular catalysts immobilized on an active catalyst support. In this case, the support not only acts as a medium for electron transfer, but also participates in the $e\text{CO}_2\text{RR}$. In this respect, Meyer and co-workers utilized the synergistic effects of the Ru^{II} polypyridyl carbene complex (RuPc) and the N-doped porous carbon (NPC) interface to steer CO_2 reduction towards C_2 products, with a particular focus on ethanol production.^[54] At -0.97 V vs. normal hydrogen electrode (NHE), a $\text{FE}_{\text{C}_2\text{H}_5\text{OH}}$ of 27.5% was obtained in 0.5 M KHCO_3 electrolyte. Considering that RuPc itself only produces CO, it was believed that the NPC support plays a key role in the C–C coupling process. First, the NPC electrode alone also reduces CO_2 to ethanol, but with a relatively low selectivity (ca. 15.0%). Second, the porous structure of NPC can enrich CO_2 or CO_2 reduction intermediates through a nanoconfinement effect, thereby facilitating C–C coupling. Therefore, it was assumed that the abundant $^*\text{CO}$ generated at the RuPc “spills over” to the RuPc/NPC interface to facilitate C–C coupling, thus significantly enhancing the selectivity for ethanol. Using the same strategy, Sargent and co-workers functionalized Cu electrodes with various porphyrin-based metallic complexes that are known to reduce CO_2 to CO.^[55] On the basis of a computational study, it was proposed that the high $^*\text{CO}$ coverage generated by the metallic porphyrin complex lowers the energy barrier for C–C coupling and thus favors the subsequent formation of $^*\text{HCCHOH}$ (ethanol path) compared with that of $^*\text{CCH}$ (ethylene pathway). Taking

5,10,15,20-tetraphenyl-21*H*,23*H*-porphine iron(III) chloride (FeTPP[Cl]) as an example, the FeTPP[Cl]/Cu catalysts achieves a CO₂-to-ethanol conversion with a FE_{C₂H₅OH} of 41 % at a partial current density of 124 mA cm⁻² in 1.0 M KHCO₃. These studies highlight the promising tandem strategy for steering the CO₂RR toward C₂₊ products by assembling molecular complexes that are active toward producing C₁ intermediates on active supports, where C–C coupling can occur. In contrast to the traditional molecular catalytic process in which the metal complex is the only active species, such tandem catalytic systems provide an alternative approach for CO₂-to-C₂₊ conversion that operates without the tedious synthesis of tailored multifunctionalized molecular catalysts. Instead, a wide range of established molecular catalysts that efficiently provide C₁ intermediates can be combined with supports that are known to promote C–C coupling.

4.3. Acetate

To enable electrochemical reduction of CO₂ to acetate, Schöfberger, Roy, and co-workers synthesized a molecular Mn^{III}-corrole complex using the same ligand as that in Figure 5A.^[56] In contrast to the previously discussed Co corrole species, Mn^{III}-corrole immobilized on carbon paper reduces CO₂ to acetic acid with a FE of 63 % and a turnover frequency (TOF) of 8.25 h⁻¹ in a moderately acidic aqueous electrolyte (pH 6). Mn^{III}-corrole is a square-planar complex and initially possesses no axial ligand coordination compared to the cobalt(III) triphenylphosphine corrole complex. Such a molecular structure renders the complex freely accessible to axial coordination by nucleophiles. A mechanism was proposed in which the CO₂ molecule first binds axially to the Mn site, followed by PCET to form a Mn-COOH intermediate. It was assumed that the Lewis acidity of the Mn^{III} center results in a strong tendency to bind to the Lewis basic carbonyl oxygen atom of the formate group, thereby facilitating C–C coupling to generate an oxalate type intermediate. The latter is eventually converted into acetate by subsequent reduction, protonation, and dehydration steps.

A further system that generates acetate was reported by Gu and co-workers. In their electrochemical study, a porphyrin-based MOF nanosheet was used as a precursor that forms a tandem system in situ during electrolysis and leads to selective eCO₂RR to acetate.^[57] The MOF consists of a porous 2D layered reticular framework with Cu porphyrin units connected through Cu₂(COO)₄ paddle wheels. It undergoes cathodized restructuring into CuO, Cu₂O, and Cu₄O₃, anchored with the Cu-porphyrin ligand. The resulting catalysts exhibit significant activity for acetate and formate production with an FE of 17 % and of 68 %, respectively, at –1.55 V vs. Ag/AgCl in an electrolyte consisting of CH₃CN as the solvent, 1 M H₂O, and 0.5 M 1-ethyl-3-methylimidazolium tetrafluoroborate.

4.4. Oxalate

The uncatalyzed electrochemical reduction of CO₂ in aprotic solvents on inert electrodes, such as carbon, mercury, and lead, produces oxalate through a coupling reaction of CO₂^{•-} radical anions by the direct reduction of CO₂ when the applied potential is sufficiently negative ($E^0_{\text{CO}_2/\text{CO}_2^{\bullet-}} = -1.97 \text{ V vs. SHE}$).^[58] In contrast to other C₂₊ products, oxalate is generated by one-electron reduction of CO₂, which does not involve any proton-transfer processes. The coupling process can also be achieved at less negative potentials using molecular catalysts. Based on the known mechanisms, homogeneously catalyzed electroreduction of CO₂ to oxalate can be divided in two categories: redox catalysis (or quasi-redox catalysis) and two-center catalysis.^[59] In redox catalytic or quasi-redox catalytic processes, the dimerization occurs between two free CO₂^{•-} radical anions produced by outer-sphere electron transfer (redox catalysis) or two-step electron transfer (quasi-redox catalysis) between CO₂ and the catalyst (Figure 6A,B). In two-center catalysis, the formation of oxalate proceeds through the dimerization of two CO₂-catalyst adducts generated by the coordination of CO₂ to the binding sites of the catalysts (Figure 6C).

It was demonstrated that a series of organic molecules (aromatic esters and nitriles, Figure 6D(i and ii)) effectively accelerate the coupling reaction, by acting as an electron mediator between the electrode and CO₂.^[60] Typically, the redox potentials of these compounds are close to that of $E^0_{\text{CO}_2/\text{CO}_2^{\bullet-}}$. It was originally assumed that the reaction is initiated by the generation of the ester or nitrile radical anion, followed by outer-sphere electron transfer from the radical anion to CO₂ and dimerization to yield oxalate. However, further investigation of the reaction kinetics revealed an inner-sphere character of the electron transfer.^[61] As depicted in Figure 6B, the transient formation of an adduct between ester or nitrile and CO₂ molecule occurs before the generation of free CO₂^{•-} radical anions, thus indicating a two-step process (quasi-redox catalysis). Despite the capability to convert CO₂ into oxalate, the method exhibits several limitations. First, as the reaction still proceeds via the high-energy CO₂^{•-} intermediate, the reaction rate depends on the unfavorable electron-transfer equilibrium between the reduced form of the catalyst and CO₂. The overpotential can, therefore, only be reduced by a few hundred mV.^[11a] Second, the organic radical anions are prone to side reactions, namely dimerization under aprotic conditions. Consequently, the catalyst concentration must be very low (1–2 mM),^[61] which greatly limits scale-up of the reaction. Third, under protic conditions, the reduced catalysts would easily degrade. Applications are thus restricted to organic aprotic solvents.

In addition to aromatic esters and nitriles, some transition-metal complexes also reduce CO₂ to oxalate at potentials close to $E^0_{\text{CO}_2/\text{CO}_2^{\bullet-}}$ through a redox or “quasi-redox” catalysis scheme. The first report focused on Ag- and Pd-based octaethylporphyrin (Figure 6D(iii)), which produces oxalate as the major product in dry dichloromethane at –1.65 V vs. Ag wire.^[62] Later, a macrocyclic [N₄²⁻] Ni

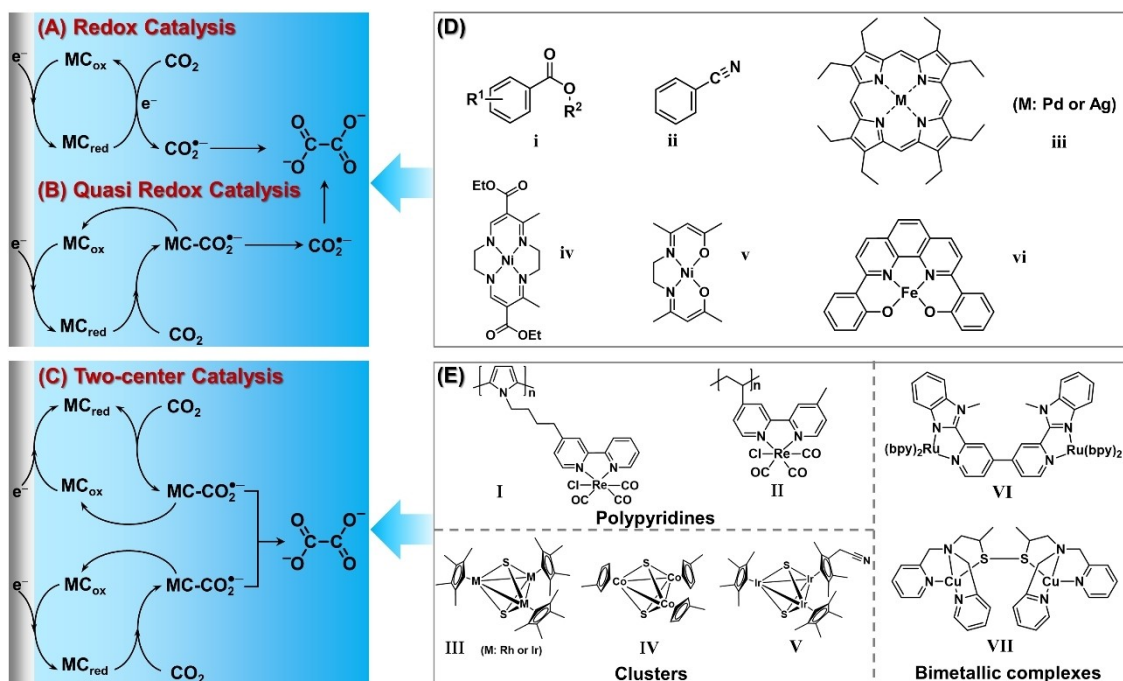


Figure 6. A–C) Proposed pathways and D, E) corresponding molecular catalysts for the formation of oxalate under $e\text{CO}_2\text{RR}$.

complex with COOEt substitution (Figure D(iv)) proved to be an efficient redox catalyst for $e\text{CO}_2\text{RR}$ to oxalate with a high FE ($>90\%$).^[63] It was assumed that the presence of a COOEt group ensures the formation of a labile metal–carbon bond through the attack of the electrophilic CO_2 at the nucleophilic metal center of the reduced complex, thus facilitating the generation of free $\text{CO}_2^{\bullet-}$ radical anions and follow-up dimerization reactions. Similarly, a $\text{Ni}^{\text{II}}\text{-}N,N'$ -ethylenebis(acetylacetoniminato) complex (Figure D(v)) electrochemically reduces CO_2 to oxalate at -2.46 V vs. Fc/Fc^+ in dry MeCN.^[64] Wong, Che, and co-workers also demonstrated a “quasi-redox” mechanism during the $e\text{CO}_2\text{RR}$ of a Fe(dophen) complex (dophen = 2,9-bis(2-hydroxyphenyl)-1,10-phenanthroline, Figure D(vi)), which produces oxalate as a minor product with FE up to 13%.^[65] In such redox or “quasi-redox” catalytic examples, the molecular design of the metal complex should consider the following key points: 1) the metal complex should be strongly electron-donating in the reduced form, thereby facilitating electron transfer to CO_2 to produce a high concentration of $\text{CO}_2^{\bullet-}$ radical anions, and 2) the metal complex should have a low Lewis acidity in the oxidized form to reduce the coordinative interaction with the $\text{CO}_2^{\bullet-}$ radical anions and promote the cleavage of the adduct.

Despite a higher reaction rate, very negative potentials are still needed in redox or “quasi-redox” catalytic processes. In contrast, two-center catalysis can generate oxalate at a much less negative potential, during which two $\text{CO}_2^{\bullet-}$ radical anions form simultaneously at different binding sites and dimerize due to the proximity of two CO_2 -metal adducts. A typical example is a polymerized film of rhenium catalysts (Figure 6E(I and II)), namely $\text{Re}(\text{bpy})(\text{CO})_3\text{Cl}$ and $\text{Re}(\text{vbpy})(\text{CO})_3\text{Cl}$ with $\text{FE}_{\text{oxalate}}$ of 15% and 5%,

respectively.^[66] The abundant molecular catalysts inside the polymerized films result in a high local concentration of metal– CO_2 adduct, which significantly enhances the probability of dimerization and oxalate formation. Tanaka and co-workers developed a series of bi- and trinuclear metal complexes with multiple binding sites. They found that trinuclear metal-sulfur clusters $[(\text{MCp}^*)(\mu_3\text{-S})_2]^{2+}$ ($\text{M}=\text{Co}, \text{Rh}, \text{Ir}$; $\text{Cp}=\text{cyclopentadienyl ring}$; Figure 6E(III–V)) catalyze $e\text{CO}_2\text{RR}$ selectively to oxalate with FEs up to 60%.^[67] Two-electron reduction of the M_3S_2 clusters caused an M–M bond cleavage, thereby creating four possible binding sites for an electrophilic attack of CO_2 , namely two coordinatively unsaturated metal sites and two $\mu_3\text{-S}$ sites. It was proposed that, as a consequence of steric shielding by the Cp^* ligands, oxalate formation proceeds in an intramolecular fashion through the coupling of two CO_2 molecules bonded to adjacent M and S atoms. Later, Tanaka and co-workers synthesized a binuclear $[\text{Ru}(\text{dmmbbpy})(\text{bpy})_2]_2$ complex (dmmbbpy = 2,2'-bis(1-methylbenzimidazol-2-yl)-4,4'-bipyridine, Figure 6E(VI)) with unsymmetrical chelating rings, which produces oxalate with a selectivity of 70% in dry MeCN.^[68] In situ IR spectra demonstrated that the oxalate generation does not result from dimerization of free $\text{CO}_2^{\bullet-}$. Two-electron reduction of the complex causes dechelation of dmmbbpy, which results in a coordinatively unsaturated Ru and monodentate dmmbbpy $^-$. The electrophilic attack of CO_2 on both binding sites facilitates a coupling reaction of CO_2 to afford oxalate.

A binuclear Cu complex (Figure 6E(VII)) reported by Bouwman and co-workers was proposed to follow a different coupling mechanism. With N -(2-mercaptopropyl)- N,N -bis(2-pyridylmethyl)amine as ligand, the two Cu sites in the complex are too remote to cooperate. Nevertheless, the

cooperation between two catalysts was proposed to enable the dimerization of two metal–CO₂ adducts but involve four CO₂ molecules. A FE of 96% was reported with a TON of 6 for the conversion of CO₂ into oxalate at a moderate potential of –0.03 V vs. NHE.^[69]

4.5. Other C₂₊ Products

Although some molecular catalysts also produce other C₂₊ products, such as glyoxal (CHO-CHO) or acetaldehyde (CH₃CHO), these compounds are usually present as minor products.^[43,53] The only exception is [Ru(bpy)(trpy)(CO)](PF₆)₂ (bpy = 2,2'-bipyridine, trpy = 2,2':6',2''-terpyridine).^[70] It can generate CHO-COOH and HOCH₂COOH at –1.75 V vs. Ag/AgCl in C₂H₅OH/H₂O (4:1 v/v). However, the C–C coupling process was realized at –20 °C, as the [Ru(bpy)(trpy)-(CO)]⁰ intermediate that is required for C–C coupling is not stable at room temperature.

5. Inducing Thermoreductive CO Coupling with Organometallic and Main Group Compounds

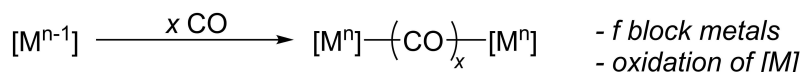
The selective molecular reductive coupling of CO to produce C₂₊ compounds by an approach other than the traditional CO hydrogenation through Fischer–Tropsch-type reactions offers an easier possibility for a detailed understanding of this fundamental transformation. Furthermore, the coupling of CO can be regarded as a model for reactions occurring during the above-mentioned reductive transformations of CO₂. This chemistry is, however, rather underdeveloped and very challenging, and has been reviewed very recently.^[71] Thus, we would like to refer the reader to these contributions for a more comprehensive and detailed overview of the field. In this section we will, therefore, only briefly discuss selected systems and instead put more emphasis on reaction principles that could guide the design of new molecular catalyst systems. Furthermore, the recent evolution from transition metal-based systems to metal-free, main group systems will be described.

In contrast to CO₂, carbon monoxide is a strong ligand for many transition metals, capable of acting either as a Lewis base through donation from its C-based lone pair of electrons or as a Lewis acid by back-bonding into its C–O π* orbital. CO is thus known to be an excellent ligand for many organometallic complexes and subsequent transformations are well-precedented in diverse carbonylation reactions, especially in combination with suitable reductants or in multimetallic systems that serve to activate CO and induce coupling. More specifically, Kong and Crimmin have identified three approaches for reductive transformations of CO,^[71a] namely a) metal-mediated reduction, b) use of external reductants, or c) reduction using sacrificial agents (Figure 7).

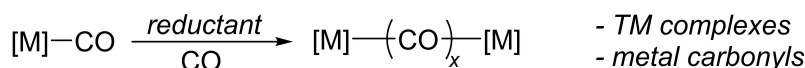
5.1. Metal-Based Complexes

The reductive coupling of CO was already observed by Liebig in 1834, who proposed the formation of “potassium carbonyl”, a compound that was later identified as a mixture of potassium ethynediolate and potassium benzenhexolate salts.^[72] From the 1980s on, several groups reported similar reactions, mediated by lanthanide, actinide, and transition metal (TM) complexes (Figure 8). At the forefront of this development were f-block complexes, likely because of their high oxophilicity and their inability to form stable carbonyl complexes.^[73] The general challenge of selectivity in CO coupling was illustrated for U complexes, where subtle changes of the substitution pattern at the cyclopentadienyl ligand in (η⁸-COT^{Si*2})(η⁵-C₅Me₄R)U(III) (COT = cyclooctatetraene, Si* = Si*Pr₃) or a variation of the reaction conditions (amount of added CO and temperature) were found to alter the nature of the product from ethynediolate to so-called deltate or squarate complexes.^[74] Related coupling reactions that involve transition-metal complexes are much rarer. An example was reported by Kays and co-workers, who observed CO coupling at Fe along with the formation of metal carbonyl and carboxylate complexes. The authors proposed involvement of the aryl group (Ar') of the FeAr'₂ precursor.^[75] Although further cases of direct CO coupling at transition-metal centers have not been reported to date,

a) Metal-mediated reduction



b) External reductants



c) Electron transfer from E–E bonds

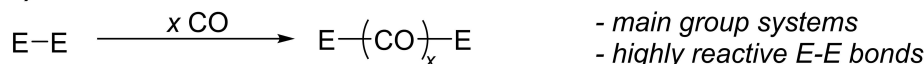


Figure 7. Reaction principles for the reductive coupling of CO.

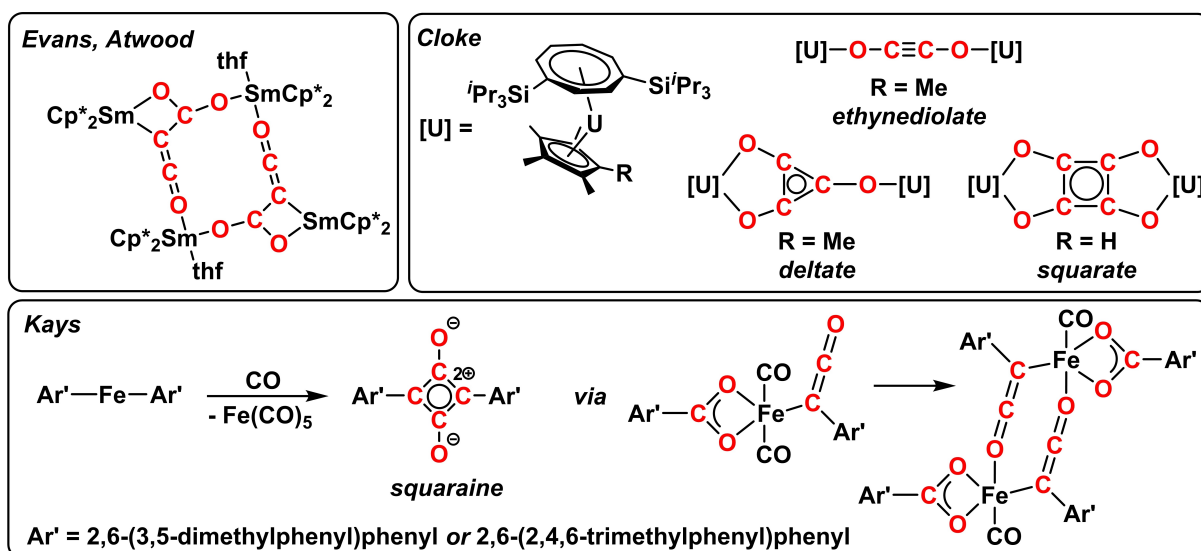


Figure 8. Selected transition-metal-based systems for the coupling of CO.

this reaction principle could be relevant for further d block metals, as it avoids the formation of carbonyl complexes.

Alternatively, electrons required for the reductive transformation of CO could be provided by an external reductant (Figure 7b). A considerable number of early to mid-transition-metal systems have been reported based on this approach, including Zr,^[76] Hf,^[77] Ta,^[78] Nb,^[79] Mo,^[80] W,^[81] Re,^[82] and Fe.^[83] In most cases, metal-coordinated CO undergoes coupling to form C₂ units with ethynediolate, alkylidene, or ketylidene complexes being important intermediates. Furthermore, the use of electrophiles that bind to the terminal O atom of the metal carbonyl unit to ultimately produce functionalized coupling products is a common principle. Although all these examples showcase the potential of this approach, which could be of great value when combined with electrochemistry, examples that go beyond the formation of C₂ products have not been reported to date.

5.2. Main Group Based Complexes

With the recent advent of main group chemistry for stoichiometric and catalytic bond activation reactions that were historically only known for transition-metal-based systems, these systems have also moved into the focus for the activation and coupling of CO (Figure 9). The direct coupling of CO (with concomitant deoxygenation) at low-valent silylene species was developed by the groups of Driess and Aldridge.^[84] In these cases, low-oxidation-state main group compounds with element–element bonds transfer electrons from the respective bonds to CO and thus induce reductive transformations.

This strategy was first reported for a dinuclear Rh^{II} porphyrin complex that inserts and couples CO between the two metal centers.^[85] Later, this approach was transferred to boryllithium compounds that possess highly polar B–Li

bonds, which is reported to be the key for the success of these transformations.^[86] Further work on main group based systems includes the Si=Si compounds developed by Scheschkewitz and co-workers that couple CO with concomitant deoxygenation via ketylidene and ethynolate intermediates^[87] and the B≡B diboryne compounds developed by Braunschweig et al. that couples CO to produce a boron-coordinated tetramer.^[88] Notably, in the latter example, the coupling of CO was confirmed to occur by an initial coordination across the B–B bond, followed by tetramerization between the boron centers in the presence of an excess of CO.

Dinuclear magnesium compounds of the type [(^ANacnac)Mg]₂ (^ANacnac = [HC(MeCNAr)₂]) are known to be well-suited for a wide range of reductive transformations.^[89] Thus, in systematic studies of the ligand influence on the selectivity in reactions with CO, Jones and co-workers observed the formation of deltate and ethynediolate complexes after desymmetrisation of the Mg dimer with Lewis base.^[90] Later, the use of additional substoichiometric amounts of Mo(CO)₆ led to the reductive hexamerization of CO to produce a Mg benzenehexolate compound,^[91] similar to that obtained two centuries ago by Liebig. In a recent concept article, the importance of transition metal impurities for this historical coupling process was discussed by Rosenthal.^[71b] Several highly interesting systems have been reported and the further rationalization of these reactivities will be crucial to move away from stoichiometric processes and to guide the design of new, potentially catalytic systems. In this respect, the incorporation of photo- and electrochemical techniques should hold great potential for this exciting field of main group chemistry.

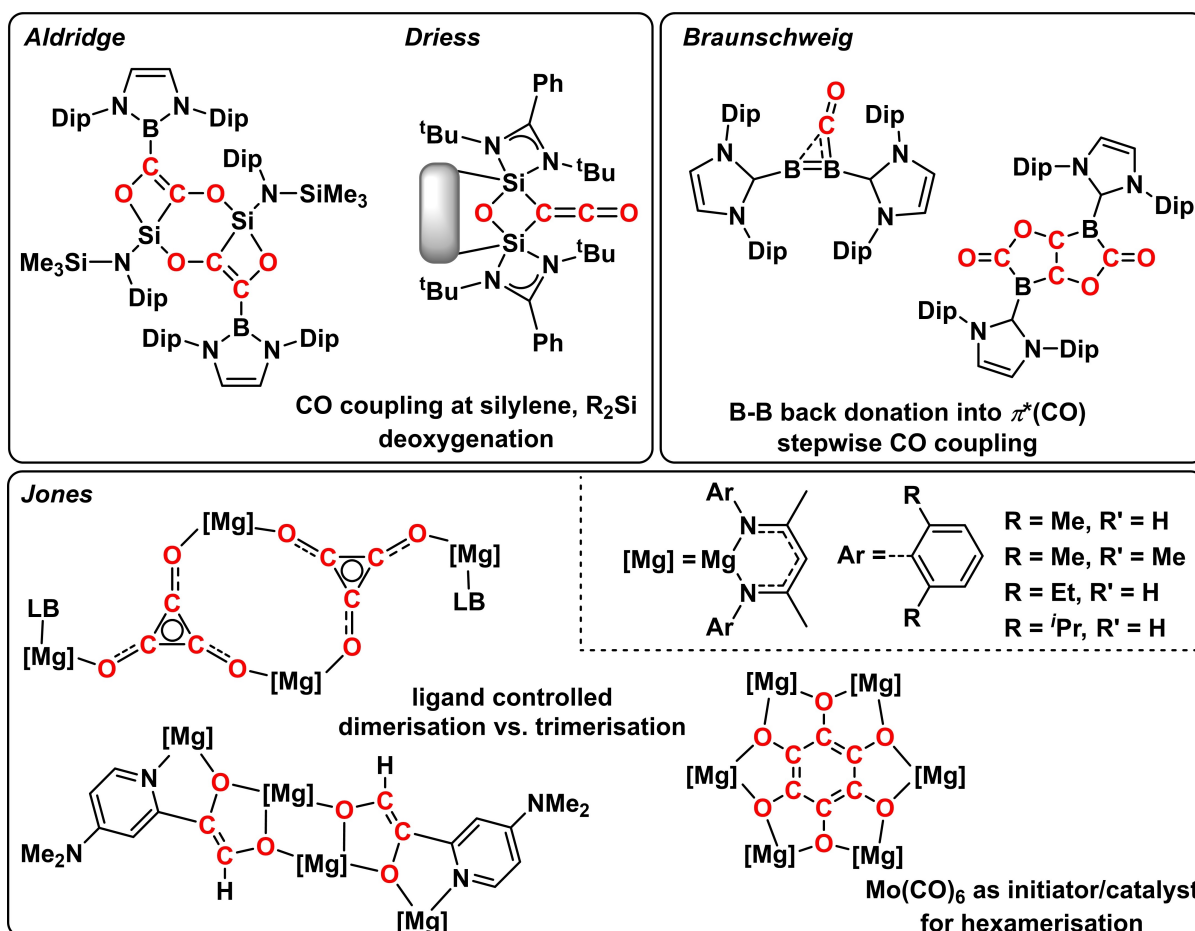


Figure 9. Selected main group based systems for the coupling of CO (Dip = 2,6-diisopropylphenyl, LB = Lewis base).

6. Conclusion and Perspectives

6.1. Issues That Need To Be Resolved

The conversion of CO_2 into higher carbon compounds by photosynthesis has inspired researchers for decades to realize this conversion in a simpler and more efficient manner. In this respect, reductive CO_2 homocoupling using (molecular) catalysts is a simple, yet fundamental transformation which continues to be a highly challenging and desirable way to produce value-added C_{2+} chemicals and fuels. More specifically, the selective formation of C_{2+} products utilizing carbon dioxide under mild reaction conditions (low temperature, no strong reductants, no significant waste formation) remains a “Holy Grail” in chemistry.

In the last few decades, interesting progress has been achieved in the formation of C–C bonds from CO_2 using molecular catalysts in reactions spanning from traditional chemical reduction to electro- and photochemical conversions. However, despite these advancements, important issues still must be resolved to enable the development of applications in the “real world”. Moreover, the mechanistic understanding of this transformation is often limited and sometimes even leads to wrong conclusions. What needs to

be done in the future to improve this coupling reaction? First, the strong binding of the metal to the carbon containing products often hampers the production of free C_{2+} compounds (product inhibition). In the non-electrochemical reductive coupling processes, most of the reported molecular catalysts generate bridging C_{2+} anionic species (particularly oxalate), in which the formed product coordinates strongly with the metal complex and cannot be easily released. It is thus of great significance to find a balance in the binding strength between the metal center and the resulting product molecules. On the one hand, the binding strength between the metal center and CO_2 (CO) should be strong enough to activate CO_2 (CO) molecules, thereby facilitating the following coupling reaction. On the other hand, the affinity of the metal center to the formed coupling product species should be relatively weak to enable the liberation of the C_{2+} compounds. A systematic investigation of the scaling relation between these two binding energies is necessary to find suitable metal centers. In this context, further opportunities lie in the tuning of the electronic properties of the catalyst by variation of the functional groups that are attached to the ligand.

Special attention should also be paid to the use of suitable orthogonal analytical methods, especially when oxalate is the product. Recently, during investigations of the

reductive dimerization of carbon dioxide, we faced significant problems and observed common pitfalls in previous studies. More specifically, we identified irreproducibility as a result of insufficient analysis and misleading analytical data in established procedures for CO₂ reduction to oxalate.^[92] In general, special attention should be paid to issues with oxalate quantification. If the generated oxalate precipitates as a salt from the reaction mixture, the quantification can be realized gravimetrically. In the case of soluble oxalate species, a number of chromatographic methods can be used, including high-performance liquid chromatography, ionic chromatography, and capillary electrophoresis. Titration with potassium permanganate is another option for oxalate quantification, although a tedious post-electrolysis treatment is required. It should be noted that the sensitivity and detection limits vary a lot between the different methods, thus extra caution is needed for performance comparison.

Another point is the stability of the molecular catalysts, which is of utmost importance for determining the real active site and potential practical applications. As described in Section 4.1, immobilized molecular catalysts may undergo reversible (or irreversible) reconstruction during eCO₂RR. The formed metal nanoclusters surrounded by the ligands may constitute the real active sites, which are responsible for the formation of C₂₊ products. Such a lack of stability certainly makes the mechanistic study more challenging, but may at the same time also lead to unexpected discoveries such as the formation of well-defined catalytically active nanoclusters. However, when eCO₂RR catalyzed by metal complexes is intended, a careful catalyst design is needed to prevent degradation during electrolysis and to ensure a stable long-term performance. First, the ligand itself should be stable enough to impede the structure change during electrolysis. Second, the metal ion/ligand binding affinity should be large enough, increase the threshold potential of the demetalation process, and thus enhance the structural stability. Substitution of the ligands with electron-donating or -withdrawing functional groups has a great influence on the stability of the metal complex, as exemplified in the cases of Cu–Pc and Co corrole macrocycles.

A comparison of molecular catalysts and heterogeneous metallic catalysts shows that the former are generally more selective for specific products because of their well-defined active centers. However, the studies available so far indicate that molecular catalysts do not display any advantage in the case of eCO₂RR with respect to the formation of C₂₊ products. It rather appears as if the same challenges associated with metallic catalysts are encountered, namely, low selectivity for specific products and accompanying generation of several C₂₊ products. Up to now, the best selectivity obtained for ethylene, ethanol, and acetate using molecular catalysts are 50 %, 48 %, and 63 %, respectively,^[45,53,56] which is still far away from the practical requirements. In addition, the production of one C₂₊ compound is usually accompanied by other C₂₊ compounds with comparable selectivity. For example, Co-corrole produces 48 % ethanol as the major product, but acetate is also generated as a minor product with FE of 10 %.^[53] Usually, the pathways to these C₂₊ compounds share several

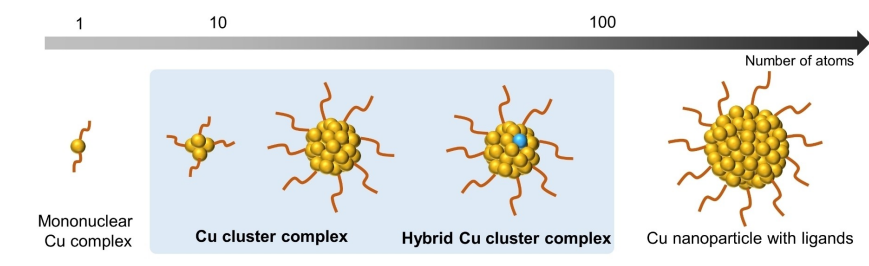
identical intermediates, and branch upon further reduction. To realize the selective production of a specific C₂₊ compound, a careful design of both the active center and the properties of the support (including the morphology) is necessary to tune the proton availability and stabilize specific intermediates at the late stage of the eCO₂RR.

6.2. Promising Strategies for C–C Coupling

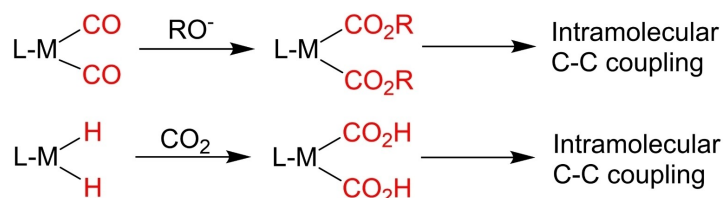
Despite the above-mentioned challenges and problems, significant progress has been made on molecular catalysts for the reductive homocoupling of CO₂ towards C₂₊ compounds, and there are many more opportunities waiting to be targeted. Considering that ligand-stabilized metal nanoclusters generated by the reversible demetalation of molecular catalysts can reduce CO₂ to C₂₊ products, it appears promising to design and synthesize further metal cluster complexes with ≥ 2 metal atoms (Figure 10A). The metal cluster cores are up to 2 nm (<ca. 100 atoms) in size, thus ensuring properties distinct from their corresponding bulk metals. The adjacent metal atoms should be in proximity to each other, allowing the coupling of two intermediates absorbed on each metal center. Thus, such metal clusters mimic the behavior of metallic electrodes, while retaining the well-defined structure characteristics of molecular catalysts. Such systems are very promising in regard to both product selectivity and mechanistic investigations. In addition, by introducing a nonsymmetric ligand sphere, it is possible to realize nanoclusters with metals in different oxidation states, which in one case was already demonstrated to favor C–C coupling.^[93] Moreover, hybrid metal cluster cores constitute interesting subjects of study (Figure 10A). Such nanoparticles can, for example, be synthesized by replacing one of the Cu atoms in a Cu cluster with another metal atom such as Ag, Au, or Zn. Such a bimetallic system may be capable of mimicking the heterogeneous bimetallic tandem systems that were found to favor the production of ethylene or ethanol.^[94] At this stage, several Cu cluster complexes are already known, although none of them have yet been tested in the CO₂RR.^[95] The challenge is the stability of these Cu cluster complexes when applied to eCO₂RR. For this purpose, the design of suitable ligands with strong binding capability offers interesting opportunities. For example, a promising starting point is represented by a recent study by Yuan et al., in which an all-amidinate-protected gold nanocluster (amidinate = *N,N'*-diphenylformamidinate) was shown to exhibit robust catalytic performance for the electroreduction of CO₂ to CO.^[96]

Another interesting strategy that, to the best of our knowledge, has not yet been put into practice, is the design of catalysts that can be converted into metalla-dicarbonyl (carboxylate) intermediates that undergo intramolecular C–C coupling. Two possible routes are conceivable for generating dicarboxylate model intermediates (Figure 10B): a) Addition of nucleophiles (OH[−] or RO[−]) to the corresponding carbonyl complexes and b) insertion of CO₂ into the corresponding hydrides. For the latter reaction, the regioselectivity of the insertion process to give the M–CO₂H

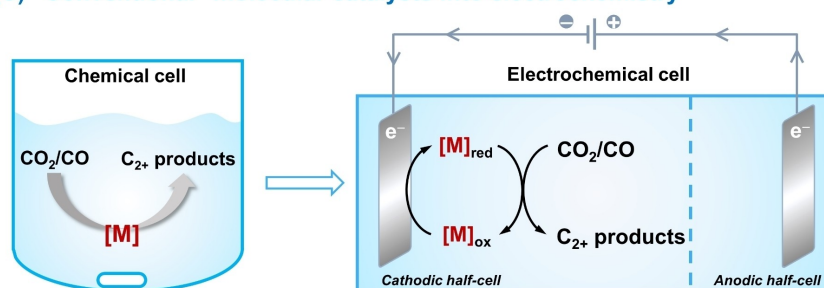
(A) Cu cluster complex



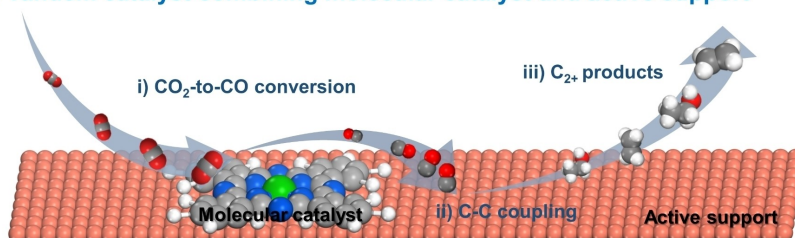
(B) Design of novel molecular catalysts



(C) “Conventional” molecular catalysts into electrochemistry



(D) Tandem catalyst combining molecular catalyst and active support



(E) Tandem reaction system

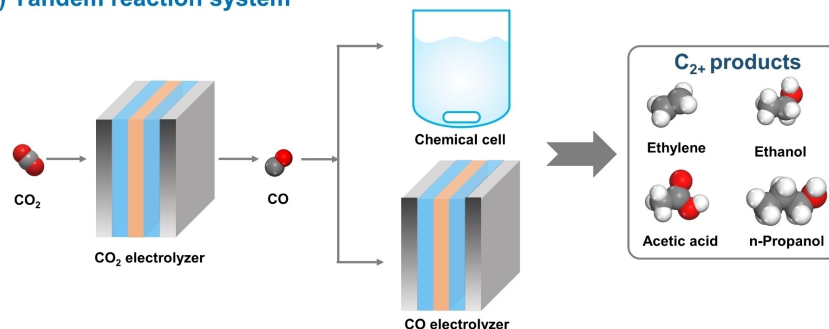


Figure 10. Promising strategies for C–C coupling. A) Design and synthesis of Cu cluster complexes. B) Design of novel molecular catalysts that are capable of forming a metalla-di(carboxylate) intermediate which can undergo intramolecular C–C coupling (here, possible synthetic routes to model intermediates are shown). C) Transforming “conventional” molecular catalysts into electrochemical ones. D) Tandem catalysis by combining a molecular catalyst with an active support. E) Tandem reaction system for CO₂ conversion to multicarbon products.

instead of the formate complex M–OCHO has to be controlled. The reactivity of the generated di(carboxylate) complex in the presence of reductants needs to be evaluated for potential C–C coupling reactions. The synthesis of such model intermediates and further conversion through intramolecular C–C bond formation could help to achieve a mechanistic understanding and, ultimately, to establish a catalytic process.

Considering that the non-electrochemical reductive coupling of CO₂ or CO by some molecular catalysts can generate the corresponding dimer, trimer, or even oligomers, it would be interesting to investigate these systems electro- or photochemically (Figure 10C). This kind of transformation is without doubt a challenging task, during which a set of rules and preconditions would have to be considered. In principle, the reduction potential of the catalyst needs to be in the appropriate range for CO₂ (CO) reduction, while the reduced form of the catalyst has to be sufficiently stable, and the chemical step must be feasible under the desired electrolysis conditions (reaction medium, temperature, etc.).^[11a]

Another promising strategy to enable reductive CO₂ coupling based on molecular catalysts is to utilize an active support material. Previously, most of the heterogeneous molecular catalysts were immobilized onto carbonaceous materials, namely carbon nanotubes, carbon black, etc. Usually, these materials do not directly participate in the CO₂RR process, and rather act as a support for the uniform dispersion of molecular catalysts and a contact medium for fast electron transfer. In this regard, the use of active support materials offers interesting opportunities to realize tandem catalysis, in which the molecular catalysts generate a high concentration of *CO, while the active supports promote C–C coupling to generate C₂₊ products (Figure 10D). Rationalization of the tandem catalytic system, based on matched potential ranges for CO generation and C–C coupling, as well as a careful design of the interface between the molecular catalysts and the active support, will be necessary to achieve optimal synergistic effects.

Similarly, tandem reaction systems are also a promising alternative to be explored.^[97] Unlike tandem catalysts that induce two-step reactions in a single cell, tandem reaction systems are designed to facilitate two-step CO₂ reductions in two separate cells with different sets of reaction conditions. A promising set-up would comprise electrochemical conversion of CO₂ into CO by suitable molecular catalysts in the first step, followed by coupling of CO to generate C₂₊ compounds (Figure 10E). The CO coupling reaction can be realized either by thermochemical or electrocatalytic reduction. Such a two-step strategy ensures more flexibility regarding the choice of catalysts and adjustment of the reaction conditions, thereby providing more possibilities of converting CO₂ into value-added chemicals.

Despite various challenges associated with reductive coupling of carbon dioxide, we believe that this research area offers not only potential for a fundamental understanding of the reactivity of carbon dioxide, but will also be of significant industrial relevance on the way to a circular economy. One of the apparently simplest C–C bond

formations certainly deserves more attention, and we need both a detailed mechanistic understanding, to provide the basis for the design of suitable catalysts, as well as completely new approaches which hopefully will provide alternative guiding principles for the construction of C₂₊ compounds from carbon dioxide.

Acknowledgements

H.-Q.L. is grateful for a Feodor-Lynen Fellowship (Alexander von Humboldt Foundation). R.F. acknowledges financial support by the DFG Heisenberg Program (FR 3848/4-1). Open Access funding enabled and organized by Projekt DEAL.

Conflict of Interest

The authors declare no conflict of interest.

Keywords: CO Homocoupling · CO₂ Homocoupling · Electrochemical Reduction · Molecular Catalyst · Thermochemical Reduction

- [1] W. Leitner, M. Schmitz, *Faraday Discuss.* **2021**, *230*, 413–426.
- [2] M. G. Kibria, J. P. Edwards, C. M. Gabardo, C.-T. Dinh, A. Seifitokaldani, D. Sinton, E. H. Sargent, *Adv. Mater.* **2019**, *31*, 1807166.
- [3] a) T. Haas, R. Krause, R. Weber, M. Demler, G. Schmid, *Nat. Catal.* **2018**, *1*, 32–39; b) B. Zhang, L. Sun, *Chem. Soc. Rev.* **2019**, *48*, 2216–2264; c) R. Daiyan, I. MacGill, R. Amal, *ACS Energy Lett.* **2020**, *5*, 3843–3847.
- [4] J. Yu, J. Wang, Y. Ma, J. Zhou, Y. Wang, P. Lu, J. Yin, R. Ye, Z. Zhu, Z. Fan, *Adv. Funct. Mater.* **2021**, *31*, 2102151.
- [5] L. J. Farrugia, S. Lopinski, P. A. Lovatt, R. D. Peacock, *Inorg. Chem.* **2001**, *40*, 558–559.
- [6] D. Gao, R. M. Arán-Ais, H. S. Jeon, B. Roldan Cuenya, *Nat. Catal.* **2019**, *2*, 198–210.
- [7] L. Rotundo, R. Gobetto, C. Nervi, *Curr. Opin. Green Sustain. Chem.* **2021**, *31*, 100509.
- [8] E. Boutin, M. Robert, *Trends Chem.* **2021**, *3*, 359–372.
- [9] a) L. Wang, S. A. Nitopi, E. Bertheussen, M. Orazov, C. G. Morales-Guio, X. Liu, D. C. Higgins, K. Chan, J. K. Nørskov, C. Hahn, T. F. Jaramillo, *ACS Catal.* **2018**, *8*, 7445–7454; b) T.-T. Zhuang, Y. Pang, Z.-Q. Liang, Z. Wang, Y. Li, C.-S. Tan, J. Li, C. T. Dinh, P. De Luna, P.-L. Hsieh, T. Burdyny, H.-H. Li, M. Liu, Y. Wang, F. Li, A. Proppe, A. Johnston, D.-H. Nam, Z.-Y. Wu, Y.-R. Zheng, A. H. Ip, H. Tan, L.-J. Chen, S.-H. Yu, S. O. Kelley, D. Sinton, E. H. Sargent, *Nat. Catal.* **2018**, *1*, 946–951.
- [10] S. Hu, T. Shima, Z. Hou, *J. Am. Chem. Soc.* **2020**, *142*, 19889–19894.
- [11] a) R. Francke, B. Schille, M. Roemelt, *Chem. Rev.* **2018**, *118*, 4631–4701; b) K. Elouarzaki, V. Kannan, V. Jose, H. S. Sabharwal, J.-M. Lee, *Adv. Energy Mater.* **2019**, *9*, 1900090; c) X.-M. Hu, S. U. Pedersen, K. Daasbjerg, *Curr. Opin. Electrochem.* **2019**, *15*, 148–154; d) L. Sun, V. Reddu, A. C. Fisher, X. Wang, *Energy Environ. Sci.* **2020**, *13*, 374–403; e) N. W. Kinzel, C. Werlé, W. Leitner, *Angew. Chem. Int. Ed.* **2021**, *60*, 11628–11686; *Angew. Chem.* **2021**, *133*, 11732–11792.

- [12] E. E. Benson, C. P. Kubiak, A. J. Sathrum, J. M. Smieja, *Chem. Soc. Rev.* **2009**, *38*, 89–99.
- [13] W. J. Evans, C. A. Seibel, J. W. Ziller, *Inorg. Chem.* **1998**, *37*, 770–776.
- [14] a) A. Paparo, J. S. Silvia, C. E. Kefalidis, T. P. Spaniol, L. Maron, J. Okuda, C. C. Cummins, *Angew. Chem. Int. Ed.* **2015**, *54*, 9115–9119; *Angew. Chem.* **2015**, *127*, 9243–9247; b) J. Lan, T. Liao, T. Zhang, L. W. Chung, *Inorg. Chem.* **2017**, *56*, 6809–6819.
- [15] A. A. Peterson, F. Abild-Pedersen, F. Studt, J. Rossmeisl, J. K. Nørskov, *Energy Environ. Sci.* **2010**, *3*, 1311–1315.
- [16] Y. Y. Birdja, E. Pérez-Gallent, M. C. Figueiredo, A. J. Göttle, F. Calle-Vallejo, M. T. M. Koper, *Nat. Energy* **2019**, *4*, 732–745.
- [17] J. H. Montoya, C. Shi, K. Chan, J. K. Nørskov, *J. Phys. Chem. Lett.* **2015**, *6*, 2032–2037.
- [18] a) E. Pérez-Gallent, M. C. Figueiredo, F. Calle-Vallejo, M. T. M. Koper, *Angew. Chem. Int. Ed.* **2017**, *56*, 3621–3624; *Angew. Chem.* **2017**, *129*, 3675–3678; b) Y. Zheng, A. Vasileff, X. Zhou, Y. Jiao, M. Jaroniec, S.-Z. Qiao, *J. Am. Chem. Soc.* **2019**, *141*, 7646–7659.
- [19] Y. Zhou, B. S. Yeo, *J. Mater. Chem. A* **2020**, *8*, 23162–23186.
- [20] H.-O. Fröhlich, H. Schreer, *Z. Chem.* **1983**, *23*, 348–349.
- [21] B. Horn, C. Limberg, C. Herwig, B. Braun, *Chem. Commun.* **2013**, *49*, 10923–10925.
- [22] B. J. Cook, G. N. Di Francesco, K. A. Abboud, L. J. Murray, *J. Am. Chem. Soc.* **2018**, *140*, 5696–5700.
- [23] N. Tsoareas, L. Castro, A. F. R. Kilpatrick, F. G. N. Cloke, L. Maron, *Chem. Sci.* **2014**, *5*, 3777–3788.
- [24] A. Yin, X. Guo, W. Dai, K. Fan, *Chem. Commun.* **2010**, *46*, 4348–4350.
- [25] W. J. Evans, S. E. Lorenz, J. W. Ziller, *Inorg. Chem.* **2009**, *48*, 2001–2009.
- [26] A.-C. Schmidt, F. W. Heinemann, C. E. Kefalidis, L. Maron, P. W. Roesky, K. Meyer, *Chem. Eur. J.* **2014**, *20*, 13501–13506.
- [27] C. J. Inman, A. S. P. Frey, A. F. R. Kilpatrick, F. G. N. Cloke, S. M. Roe, *Organometallics* **2017**, *36*, 4539–4545.
- [28] A. Klose, J. Heschbrouck, E. Solari, M. Latronico, C. Floriani, N. Re, A. Chiesi-Villa, C. Rizzoli, *J. Organomet. Chem.* **1999**, *591*, 45–62.
- [29] R. T. Stibrany, H. J. Schugar, J. A. Potenza, *Acta Crystallogr. Sect. E* **2005**, *61*, m1904–m1906.
- [30] C. T. Saouma, C. C. Lu, M. W. Day, J. C. Peters, *Chem. Sci.* **2013**, *4*, 4042–4051.
- [31] T. T. Adamson, S. P. Kelley, W. H. Bernskoetter, *Organometallics* **2020**, *39*, 3562–3571.
- [32] A. J. Boutland, I. Pernik, A. Stasch, C. Jones, *Chem. Eur. J.* **2015**, *21*, 15749–15758.
- [33] J. Li, M. Hermann, G. Frenking, C. Jones, *Angew. Chem. Int. Ed.* **2012**, *51*, 8611–8614; *Angew. Chem.* **2012**, *124*, 8739–8742.
- [34] C. Weetman, P. Bag, T. Szilvási, C. Jandl, S. Inoue, *Angew. Chem. Int. Ed.* **2019**, *58*, 10961–10965; *Angew. Chem.* **2019**, *131*, 11077–11081.
- [35] a) S. Oh, J. R. Gallagher, J. T. Miller, Y. Surendranath, *J. Am. Chem. Soc.* **2016**, *138*, 1820–1823; b) X. Qiao, Q. Li, R. N. Schaugaard, B. W. Noffke, Y. Liu, D. Li, L. Liu, K. Raghavachari, L.-s. Li, *J. Am. Chem. Soc.* **2017**, *139*, 3934–3937.
- [36] a) C. W. Machan, M. D. Sampson, C. P. Kubiak, *J. Am. Chem. Soc.* **2015**, *137*, 8564–8571; b) M.-N. Collomb-Dunand-Sauthier, A. Deronzier, R. Ziessel, *Inorg. Chem.* **1994**, *33*, 2961–2967.
- [37] a) M. Bourrez, F. Molton, S. Chardon-Noblat, A. Deronzier, *Angew. Chem. Int. Ed.* **2011**, *50*, 9903–9906; *Angew. Chem.* **2011**, *123*, 10077–10080; b) C. Steinlechner, A. F. Roesel, E. Oberem, A. Pöpcke, N. Rockstroh, F. Gloaguen, S. Lochbrunner, R. Ludwig, A. Spannenberg, H. Junge, R. Francke, M. Beller, *ACS Catal.* **2019**, *9*, 2091–2100; c) F. Franco, C. Cometto, L. Nencini, C. Barolo, F. Sordello, C. Minero, J. Fiedler, M. Robert, R. Gobetto, C. Nervi, *Chem. Eur. J.* **2017**, *23*, 4782–4793.
- [38] a) P. Kang, T. J. Meyer, M. Brookhart, *Chem. Sci.* **2013**, *4*, 3497–3502; b) P. Kang, C. Cheng, Z. Chen, C. K. Schauer, T. J. Meyer, M. Brookhart, *J. Am. Chem. Soc.* **2012**, *134*, 5500–5503.
- [39] a) E. Oberem, A. F. Roesel, A. Rosas-Hernández, T. Kull, S. Fischer, A. Spannenberg, H. Junge, M. Beller, R. Ludwig, M. Roemelt, R. Francke, *Organometallics* **2019**, *38*, 1236–1247; b) A. Rosas-Hernández, H. Junge, M. Beller, M. Roemelt, R. Francke, *Catal. Sci. Technol.* **2017**, *7*, 459–465.
- [40] a) X.-M. Hu, M. H. Rønne, S. U. Pedersen, T. Skrydstrup, K. Daasbjerg, *Angew. Chem. Int. Ed.* **2017**, *56*, 6468–6472; *Angew. Chem.* **2017**, *129*, 6568–6572; b) S. Ren, D. Joulié, D. Salvatore, K. Torbensen, M. Wang, M. Robert, C. P. Berlinguette, *Science* **2019**, *365*, 367–369; c) E. Boutin, L. Merakeb, B. Ma, B. Boudry, M. Wang, J. Bonin, E. Anxolabéhère-Mallart, M. Robert, *Chem. Soc. Rev.* **2020**, *49*, 5772–5809.
- [41] T. V. Magdesieva, T. Yamamoto, D. A. Tryk, A. Fujishima, *J. Electrochem. Soc.* **2002**, *149*, D89.
- [42] Z. Weng, J. Jiang, Y. Wu, Z. Wu, X. Guo, K. L. Materna, W. Liu, V. S. Batista, G. W. Brudvig, H. Wang, *J. Am. Chem. Soc.* **2016**, *138*, 8076–8079.
- [43] S. Kusama, T. Saito, H. Hashiba, A. Sakai, S. Yotsuhashi, *ACS Catal.* **2017**, *7*, 8382–8385.
- [44] M. Balamurugan, H.-Y. Jeong, V. S. K. Choutipalli, J. S. Hong, H. Seo, N. Saravanan, J. H. Jang, K.-G. Lee, Y. H. Lee, S. W. Im, V. Subramanian, S. H. Kim, K. T. Nam, *Small* **2020**, *16*, 2000955.
- [45] X.-F. Qiu, H.-L. Zhu, J.-R. Huang, P.-Q. Liao, X.-M. Chen, *J. Am. Chem. Soc.* **2021**, *143*, 7242–7246.
- [46] a) Y. Li, H. Wang, L. Xie, Y. Liang, G. Hong, H. Dai, *J. Am. Chem. Soc.* **2011**, *133*, 7296–7299; b) X. Zou, X. Huang, A. Goswami, R. Silva, B. R. Sathe, E. Mikmeková, T. Asefa, *Angew. Chem. Int. Ed.* **2014**, *53*, 4372–4376; *Angew. Chem.* **2014**, *126*, 4461–4465.
- [47] X. Zhang, Z. Wu, X. Zhang, L. Li, Y. Li, H. Xu, X. Li, X. Yu, Z. Zhang, Y. Liang, H. Wang, *Nat. Commun.* **2017**, *8*, 14675.
- [48] C. Guo, S. Liu, Z. Chen, B. Li, L. Chen, C. V. Singh, B. Liu, Q. Mao, *Chem. Commun.* **2021**, *57*, 1384–1387.
- [49] a) J. Wang, L. Gan, Q. Zhang, V. Reddu, Y. Peng, Z. Liu, X. Xia, C. Wang, X. Wang, *Adv. Energy Mater.* **2019**, *9*, 1803151; b) X. Han, M. Wang, M. L. Le, N. M. Bedford, T. J. Woehl, V. S. Thoi, *Electrochim. Acta* **2019**, *297*, 545–552.
- [50] Z. Weng, Y. Wu, M. Wang, J. Jiang, K. Yang, S. Huo, X.-F. Wang, Q. Ma, G. W. Brudvig, V. S. Batista, Y. Liang, Z. Feng, H. Wang, *Nat. Commun.* **2018**, *9*, 415.
- [51] R. Reske, H. Mistry, F. Beharid, B. Roldan Cuenya, P. Strasser, *J. Am. Chem. Soc.* **2014**, *136*, 6978–6986.
- [52] H. Xu, D. Rebollar, H. He, L. Chong, Y. Liu, C. Liu, C.-J. Sun, T. Li, J. V. Muntean, R. E. Winans, D.-J. Liu, T. Xu, *Nat. Energy* **2020**, *5*, 623–632.
- [53] S. Gonglach, S. Paul, M. Haas, F. Pillwein, S. S. Sreejith, S. Barman, R. De, S. Müllegger, P. Gerschel, U.-P. Apfel, H. Coskun, A. Aljabour, P. Stadler, W. Schöfberger, S. Roy, *Nat. Commun.* **2019**, *10*, 3864.
- [54] Y. Liu, X. Fan, A. Nayak, Y. Wang, B. Shan, X. Quan, T. J. Meyer, *Proc. Natl. Acad. Sci. USA* **2019**, *116*, 26353.
- [55] F. Li, Y. C. Li, Z. Wang, J. Li, D.-H. Nam, Y. Lum, M. Luo, X. Wang, A. Ozden, S.-F. Hung, B. Chen, Y. Wang, J. Wicks, Y. Xu, Y. Li, C. M. Gabardo, C.-T. Dinh, Y. Wang, T.-T. Zhuang, D. Sinton, E. H. Sargent, *Nat. Catal.* **2020**, *3*, 75–82.
- [56] R. De, S. Gonglach, S. Paul, M. Haas, S. S. Sreejith, P. Gerschel, U.-P. Apfel, T. H. Vuong, J. Rabeah, S. Roy, W. Schöfberger, *Angew. Chem. Int. Ed.* **2020**, *59*, 10527–10534; *Angew. Chem.* **2020**, *132*, 10614–10621.
- [57] J.-X. Wu, S.-Z. Hou, X.-D. Zhang, M. Xu, H.-F. Yang, P.-S. Cao, Z.-Y. Gu, *Chem. Sci.* **2019**, *10*, 2199–2205.

- [58] a) I. Shoichiro, T. Takehiko, I. Kaname, *Bull. Chem. Soc. Jpn.* **1987**, *60*, 2517–2522; b) B. R. Eggins, E. M. Brown, E. A. McNeill, J. Grimshaw, *Tetrahedron Lett.* **1988**, *29*, 945–948.
- [59] J.-M. Savéant, *Chem. Rev.* **2008**, *108*, 2348–2378.
- [60] G. Filardo, S. Gambino, G. Silvestri, A. Gennaro, E. Vianello, *J. Electroanal. Chem. Interfacial Electrochem.* **1984**, *177*, 303–309.
- [61] A. Gennaro, A. A. Isse, J.-M. Savéant, M.-G. Severin, E. Vianello, *J. Am. Chem. Soc.* **1996**, *118*, 7190–7196.
- [62] J. Y. Becker, B. Vainas, R. Eger, L. Kaufman, *J. Chem. Soc. Chem. Commun.* **1985**, 1471–1472.
- [63] M. Rudolph, S. Dautz, E.-G. Jäger, *J. Am. Chem. Soc.* **2000**, *122*, 10821–10830.
- [64] M. Y. Udugala-Ganehenege, N. M. Dissanayake, Y. Liu, A. M. Bond, J. Zhang, *Transition Met. Chem.* **2014**, *39*, 819–830.
- [65] S.-N. Pun, W.-H. Chung, K.-M. Lam, P. Guo, P.-H. Chan, K.-Y. Wong, C.-M. Che, T.-Y. Chen, S.-M. Peng, *J. Chem. Soc. Dalton Trans.* **2002**, 575–583.
- [66] a) T. R. O'Toole, B. P. Sullivan, M. R. M. Bruce, L. D. Margerum, R. W. Murray, T. J. Meyer, *J. Electroanal. Chem. Interfacial Electrochem.* **1989**, *259*, 217–239; b) S. Cosnier, A. Deronzier, J.-C. Moutet, *J. Electroanal. Chem. Interfacial Electrochem.* **1986**, *207*, 315–321.
- [67] a) Y. Kushi, H. Nagao, T. Nishioka, K. Isobe, K. Tanaka, *Chem. Lett.* **1994**, *23*, 2175–2178; b) Y. Kushi, H. Nagao, T. Nishioka, K. Isobe, K. Tanaka, *J. Chem. Soc. Chem. Commun.* **1995**, 1223–1224; c) K. Tanaka, Y. Kushi, K. Tsuge, K. Toyohara, T. Nishioka, K. Isobe, *Inorg. Chem.* **1998**, *37*, 120–126.
- [68] M. Meser Ali, H. Sato, T. Mizukawa, K. Tsuge, M.-a. Haga, K. Tanaka, *Chem. Commun.* **1998**, 249–250.
- [69] R. Angamuthu, P. Byers, M. Lutz, A. L. Spek, E. Bouwman, *Science* **2010**, *327*, 313–315.
- [70] H. Nagao, T. Mizukawa, K. Tanaka, *Inorg. Chem.* **1994**, *33*, 3415–3420.
- [71] a) R. Y. Kong, M. R. Crimmin, *Dalton Trans.* **2020**, *49*, 16587–16597; b) U. Rosenthal, *Chem. Eur. J.* **2020**, *26*, 14507–14511.
- [72] a) J. Liebig, *Ann. Chem. Pharm.* **1834**, *11*, 182–189; b) W. Büchner, E. Weiss, *Helv. Chim. Acta* **1964**, *47*, 1415–1423.
- [73] a) W. J. Evans, J. W. Grate, L. A. Hughes, H. Zhang, J. L. Atwood, *J. Am. Chem. Soc.* **1985**, *107*, 3728–3730; b) W. J. Evans, D. S. Lee, J. W. Ziller, N. Kaltsoyannis, *J. Am. Chem. Soc.* **2006**, *128*, 14176–14184.
- [74] a) O. T. Summerscales, F. G. N. Cloke, P. B. Hitchcock, J. C. Green, N. Hazari, *J. Am. Chem. Soc.* **2006**, *128*, 9602–9603; b) A. S. Frey, F. G. N. Cloke, P. B. Hitchcock, I. J. Day, J. C. Green, G. Aitken, *J. Am. Chem. Soc.* **2008**, *130*, 13816–13817; c) N. Tsoureas, O. T. Summerscales, F. G. N. Cloke, S. M. Roe, *Organometallics* **2013**, *32*, 1353–1362.
- [75] H. R. Sharpe, A. M. Geer, L. J. Taylor, B. M. Gridley, T. J. Blundell, A. J. Blake, E. S. Davies, W. Lewis, J. McMaster, D. Robinson, D. L. Kays, *Nat. Commun.* **2018**, *9*, 3757.
- [76] a) D. H. Berry, J. E. Bercaw, A. J. Jircitano, K. B. Mertes, *J. Am. Chem. Soc.* **1982**, *104*, 4712–4715; b) F. Calderazzo, U. Englert, A. Guarini, F. Marchetti, G. Pampaloni, A. Segre, *Angew. Chem. Int. Ed. Engl.* **1994**, *33*, 1188–1189; *Angew. Chem.* **1994**, *106*, 1254–1256.
- [77] F. Calderazzo, U. Englert, A. Guarini, F. Marchetti, G. Pampaloni, A. Segre, G. Tripepi, *Chem. Eur. J.* **1996**, *2*, 412–419.
- [78] P. A. Bianconi, I. D. Williams, M. P. Engeler, S. J. Lippard, *J. Am. Chem. Soc.* **1986**, *108*, 311–313.
- [79] P. A. Bianconi, R. N. Vrtis, C. P. Rao, I. D. Williams, M. P. Engeler, S. J. Lippard, *Organometallics* **1987**, *6*, 1968–1977.
- [80] J. A. Buss, T. Agapie, *Nature* **2016**, *529*, 72–75.
- [81] R. Y. Kong, M. R. Crimmin, *J. Am. Chem. Soc.* **2018**, *140*, 13614–13617.
- [82] R. Yadav, T. Simler, M. T. Gamer, R. Köppe, P. W. Roesky, *Chem. Commun.* **2019**, 55, 5765–5768.
- [83] D. L. M. Suess, J. C. Peters, *J. Am. Chem. Soc.* **2013**, *135*, 12580–12583.
- [84] a) Y. Wang, A. Kostenko, T. J. Hadlington, M.-P. Luecke, S. Yao, M. Driess, *J. Am. Chem. Soc.* **2019**, *141*, 626–634; b) A. V. Protchenko, P. Vasko, D. C. H. Do, J. Hicks, M. Á. Fuentes, C. Jones, S. Aldridge, *Angew. Chem. Int. Ed.* **2019**, *58*, 1808–1812; *Angew. Chem.* **2019**, *131*, 1822–1826.
- [85] B. B. Wayland, A. E. Sherry, V. L. Coffin, *J. Chem. Soc. Chem. Commun.* **1989**, 662–663.
- [86] a) W. Lu, H. Hu, Y. Li, R. Ganguly, R. Kinjo, *J. Am. Chem. Soc.* **2016**, *138*, 6650–6661; b) B. Wang, G. Luo, M. Nishiura, Y. Luo, Z. Hou, *J. Am. Chem. Soc.* **2017**, *139*, 16967–16973.
- [87] M. Majumdar, I. Omlor, C. B. Yildiz, A. Azizoglu, V. Huch, D. Scheschke, *Angew. Chem. Int. Ed.* **2015**, *54*, 8746–8750; *Angew. Chem.* **2015**, *127*, 8870–8874.
- [88] H. Braunschweig, T. Dellermann, R. D. Dewhurst, W. C. Ewing, K. Hammond, J. O. C. Jimenez-Halla, T. Kramer, I. Krummenacher, J. Mies, A. K. Phukan, A. Vargas, *Nat. Chem.* **2013**, *5*, 1025–1028.
- [89] C. Jones, *Nat. Chem. Rev.* **2017**, *1*, 0059.
- [90] a) K. Yuvaraj, I. Douair, A. Paparo, L. Maron, C. Jones, *J. Am. Chem. Soc.* **2019**, *141*, 8764–8768; b) K. Yuvaraj, I. Douair, D. D. L. Jones, L. Maron, C. Jones, *Chem. Sci.* **2020**, *11*, 3516–3522.
- [91] A. Paparo, K. Yuvaraj, A. J. R. Matthews, I. Douair, L. Maron, C. Jones, *Angew. Chem. Int. Ed.* **2021**, *60*, 630–634; *Angew. Chem.* **2021**, *133*, 640–644.
- [92] M. Marx, H. Frauendorf, A. Spannenberg, H. Neumann, M. Beller, *JACS Au* **2022**, *2*, <http://doi.org/10.1021/jacsau.2c00005>.
- [93] X. Bai, Q. Li, L. Shi, X. Niu, C. Ling, J. Wang, *Small* **2020**, *16*, 1901981.
- [94] C. G. Morales-Guio, E. R. Cave, S. A. Nitopi, J. T. Feaster, L. Wang, K. P. Kuhl, A. Jackson, N. C. Johnson, D. N. Abram, T. Hatsukade, C. Hahn, T. F. Jaramillo, *Nat. Catal.* **2018**, *1*, 764–771.
- [95] a) M. S. Ziegler, K. V. Lakshmi, T. D. Tilley, *J. Am. Chem. Soc.* **2017**, *139*, 5378–5386; b) M. Olaru, E. Rychagova, S. Ketkov, Y. Shynkarenko, S. Yakunin, M. V. Kovalenko, A. Yablonskiy, B. Andreev, F. Kleemiss, J. Beckmann, M. Vogt, *J. Am. Chem. Soc.* **2020**, *142*, 373–381; c) A. W. Cook, Z. R. Jones, G. Wu, S. L. Scott, T. W. Hayton, *J. Am. Chem. Soc.* **2018**, *140*, 394–400.
- [96] S.-F. Yuan, R.-L. He, X.-S. Han, J.-Q. Wang, Z.-J. Guan, Q.-M. Wang, *Angew. Chem. Int. Ed.* **2021**, *60*, 14345–14349; *Angew. Chem.* **2021**, *133*, 14466–14470.
- [97] X. Fu, J. Zhang, Y. Kang, *React. Chem. Eng.* **2021**, *6*, 612–628.

Manuscript received: January 17, 2022

Accepted manuscript online: February 21, 2022

Version of record online: March 24, 2022